12-2023

The Developmental Process for Adenoviral Vectored Canine Influenza Vaccines

Nicholas Jeanjaquet
University of Nebraska-Lincoln, njeanjaquet2@huskers.unl.edu

THE DEVELOPMENTAL PROCESS FOR ADENOVIRAL VECTORED CANINE INFLUENZA VACCINES

by

Nicholas E. Jeanjaquet

A THESIS

Presented to the Faculty of

The Graduate College at the University of Nebraska

In Partial Fulfillment of Requirements

For the Degree of Master of Science

Major: Biological Sciences

Under the Supervision of Professor Eric A. Weaver

Lincoln, Nebraska

December 2023

THE DEVEOPMENTAL PROCESS FOR ADENOVIRAL VECTORED CANINE INFLUENZA VACCINES

Nicholas E. Jeanjaquet M.S.

University of Nebraska, 2023

Advisor: Eric A. Weaver

Canine Influenza Virus (CIV) is a recently emerged branch of Influenza A virus that is highly infectious in dogs. The first strain was isolated in 2003, and it has quickly become endemic in areas with dense dog populations, most notably in Asia. The proximity of dogs to humans, along with their potential to serve as mixing vessels for reassortment, raises concern for possible zoonotic transmission and a potential human pandemic. Available vaccines are not frequently updated and struggle to prevent the spread of currently circulating strains. This highlights the need for a new and more effective vaccine. We outline the developmental process for our proposed solution to providing a more broadly protective vaccine. Initial development began by generating a computationally derived mosaic CIV hemagglutinin (CanH3 Mosaic), designed to maximize potential T cell epitopes. Delivery of this mosaic immunogen will be achieved with both human Adenovirus Type 5 (HAd5) and Canine Adenovirus Type 2 (CAV-2) vectors. Utilizing the pAdEasy vector system, our CanH3 mosaic was cloned into replication-defective HAd5. Simultaneously, we developed a series of plasmids through Gibson assembly and overlapping PCR that can potentially be used to generate recombinant CAV-2. We predict that these adenovirus vectored vaccines, delivering our

mosaic immunogen, will be able to provide broader and more durable protection than commercially available vaccines.

ACKNOWLEDGEMENTS

I would sincerely like to thank Dr. Eric Weaver for all the guidance he has offered me while under his mentorship. He was very flexible, helpful, and understanding when it came to my experience as a graduate student. I would also like to thank all the other faculty members who were there to help me learn and grow as a scientist and a person.

I am extremely grateful for the love and support that my parents have offered me through my entire education. They constantly encourage me to pursue my dreams and I will forever be grateful for it. I also want to thank Kristina Woodward for the love and support through all the hardships I faced throughout graduate school. Finally, thank you to all my friends, specifically Matt Pekarek and Erika Petro Turnquist, for being so dependable, I felt like I could rely on you guys for anything.

TABLE OF CONTENTS

LISTS OF TABLES AND FIGURES

CHAPTER 1- INTRODUCTION TO INFLUENZA VIRUS

INTRODUCTION

Influenza viruses are responsible for seasonal respiratory ailments on the world stage. Each year they cause roughly 9 to 41 million illnesses in the United States (US), leading to major health and economic impacts [1]. In 2015 alone, the economic burden of influenza reached 11.2 billion dollars [2]. Vaccination against influenza remains at the forefront of preventative measures that attempt to minimize the health and economic burden on society [3, 4]. Unfortunately, the yearly effectiveness of these vaccines varies quite drastically due to the unpredictability of these viruses [3]. Beyond seasonal epidemics, influenza also presents a constant pandemic threat. Recently, in 2009, there was a zoonotic transmission event of influenza virus from swine to humans that resulted in a global pandemic infecting approximately 24% of the world's population [5]. As influenza is directly responsible for four pandemics, it is essential to study and control influenza, to prevent another pandemic on the world stage [6].

Influenza viruses belong to the *Orthomyxoviridae* family and are divided into 4 main types, Influenza A, B, C, and D [7]. Influenza A and B are the main driving forces behind seasonal epidemics, with the former being more common, as roughly 75% of annual influenza cases can be attributed to Influenza A [8]. Influenza A is not limited to humans, as their host range includes a variety of mammalian and avian species such as dogs, pigs, common waterfowl, horses, bats, and chickens [9]. The relatively broad host range of influenza allows for a large variety and abundance of subtypes and strains to circulate through populations at a time. This poses a significant and ever-present risk of cross species transmission from several different animal reservoirs to humans [10].

STRUCTURE AND REPLICATION OF INFLUENZA

The enveloped particle of an Influenza A virus encompasses a genome comprised of eight distinct, single-stranded, negative-sense RNA segments [10]. These eight segments listed from largest to smallest are as follows: Polymerase Basic 2 (PB2) gene, Polymerase Basic 1 (PB1) gene, Polymerase acidic (PA) gene, Hemagglutinin (HA) gene, Nucleoprotein (NP) gene, Neuraminidase (NA) gene, Matrix (M) gene, and Nonstructural (NS) gene (Table 1.1) [10]. Each of these genes encode for at least one and up to four polypeptides, including the surface glycoproteins hemagglutinin (HA) required for entry of cells and neuraminidase (NA) required for exit of cells, polymerase subunits required for replication (PA, PB1, and PB2), viral nucleoprotein (NP), a matrix/membrane protein 1 and 2 (M1 and M2), nonstructural proteins (NS), and nuclear export protein (NS2 or NEP) (Table 1.1) [10, 11].

Due to their enveloped nature, the morphology of Influenza virions is flexible, leading to either a spherical or pleomorphic shape ranging from 80-100nm in size [10]. These particles house three vital proteins on the surface, HA, NA, and M2, with HA being the most abundant followed by NA [10-12]. Due to their surface exposure and high concentrations, the antigenic properties of Influenza viruses are heavily defined by their HA and NA proteins, leading to both being common immune targets. Currently there are 18 identified subtypes of HA and 11 identified subtypes of NA, which are used to classify these viruses, as each virus codes for one subtype of each protein [7]. Influenza isolates are further named by type, host (if not human), location, isolate number, and year identified [11].

Gene	Protein	Function
Polymerase Basic 2 (PB2)	PB2	Part of the vRNP complex. Component of the viral RNA-dependent RNA polymerase (vRdRp). Facilitates transport to the nucleus. Binds to 5' cap of mRNA to facilitate cap snatching.
Polymerase Basic 1 (PB1)	PB1	Part of vRNP complex Component of vRdRp responsible for elongation
	PB1-F2	Tied to Pathogenicity Induces Apoptosis
Polymerase Acidic (PA)	PA	Part of vRNP complex Component of vRdRp Endonuclease activity to bind and cleave off 5' mRNA caps.
Hemagglutinin (HA)	HA1	Globular head that facilitates binding to sialic acids
	HA2	Stem or stalk Contains fusion domain required for entry into cytoplasm
Nucleoprotein (NP)	NP	Facilitates Nuclear Import Binds and encapsulates genome
Neuraminidase (NA)	NA	Cleaves sialic acids to help facilitate release from infected cell, prevent aggregation, and penetrate mucus layers
Matrix (M)	M1	Facilitates nuclear export of vRNPs
	M2	Proton channel Facilitates Uncoating and budding
Non-structural (NS)	NS1	Inhibits IFN response
	NS2 or NEP	Facilitates nuclear export of vRNP

Table 1.1: IAV Genome Segments, Proteins, and Function. *Partially adapted from Chauhan et al 2022, this table lists each of the IAV genome segments, the major proteins they encode, and the known function of each protein [10].*

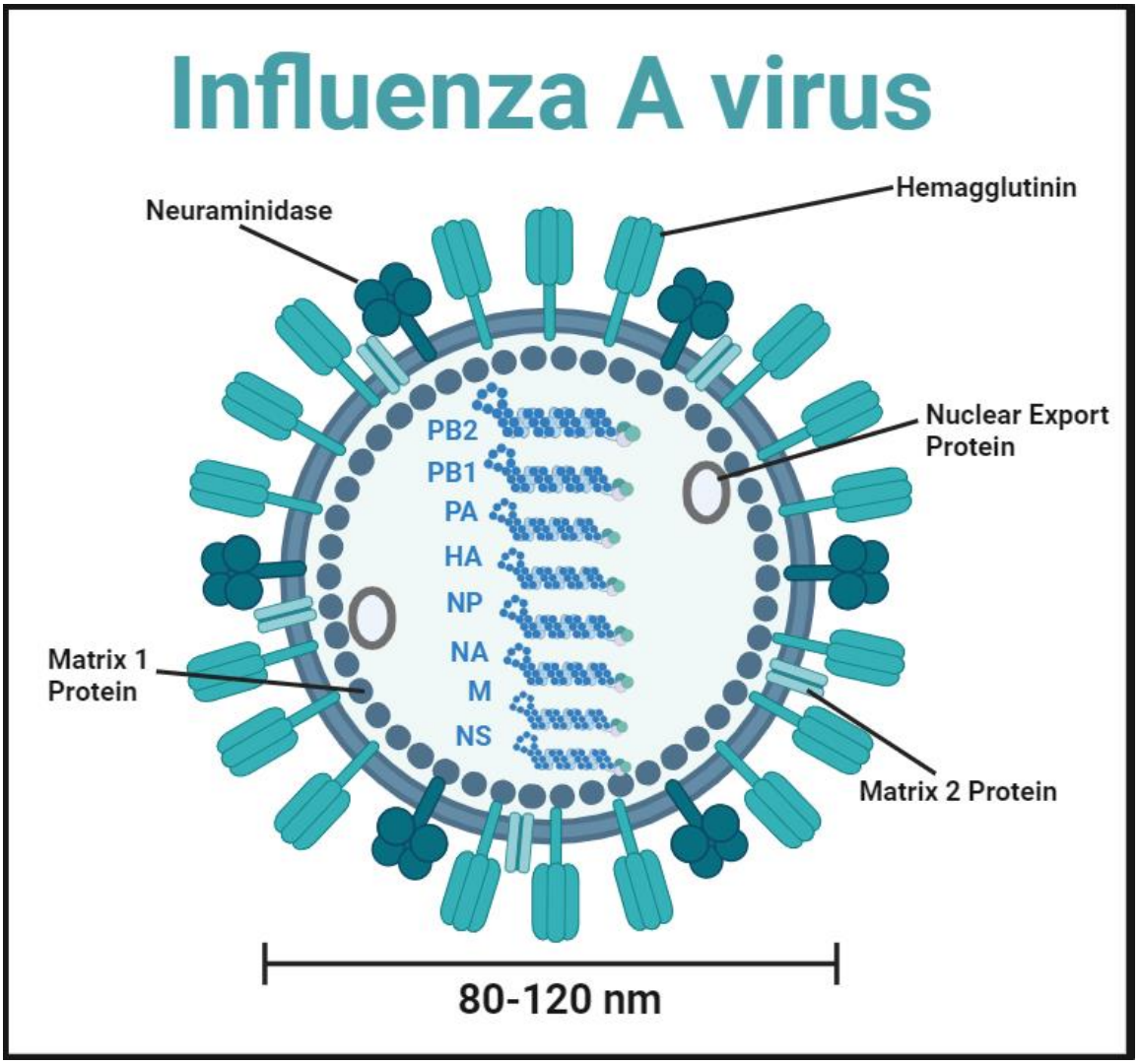

Figure 1.1: Influenza Virus Structure: *The enveloped virus particle is often depicted in spherical shape and is roughly 80-120 nm in size [11]. Within the membrane it houses 3 proteins: Hemagglutinin, Neuraminidase, and Matrix Protein 2. Hemagglutinin is the most abundant surface protein, outnumbering Neuraminidase 5-10 times [10]. Along with the 8 genome segments (PB2, PB1, PA, HA, NP, NA, M, and NS), Matrix 1 Protein (M1) and the Nuclear Export Protein (NEP or NS2) can be found inside the virion [10, 11].*

Viral entry starts with the hemagglutinin protein, which mediates viral particle binding to sialic acids bound to cell surface glycoproteins (Figure 1.2) [9, 10, 12]. HA protein exists as a homotrimer on the viral surface, with each polypeptide containing two major domains, HA1 or globular head and HA2 or stem [13]. Binding to cell surface receptors is facilitated through its HA1 subunit, while the HA2 subunit contains the fusion and transmembrane domains [10]. Epithelial cells in the respiratory tract of mammals, and in the intestinal tract of birds are the typical target cells for infection. Therefore, mammalian influenza viruses preferably bind to alpha-2,6 sialic acids, which are present at high levels in the mammalian respiratory tract, while avian influenza viruses preferably bind to alpha-2,3 sialic acids, which are present at high levels in the avian intestinal tract [9, 13]. Following binding, the viral particle will be endocytosed and acidified leading to a conformational change in HA, which exposes the fusion peptide within the HA2 subunit. This fusion peptide facilitates the fusion of the viral and endosomal membranes, releasing the viral genome segments into the cellular matrix [9, 10]. The genome segments are released as viral ribonucleoprotein complexes (vRNP) as each is bound closely by a heterotrimeric polymerase containing PA, PB1, and PB2, on the ends, and NP throughout the rest of the viral genome [14]. Nuclear localization signals (NLS) found on these bound proteins guide these vRNP complexes to the cellular nucleus [10].

Once inside the nucleus, the viral RNA polymerase initiates transcription by first cleaving cellular mRNA 10-15 nucleotides downstream of the 5’ cap [12]. Viral transcription is then primed using this capped mRNA oligonucleotide [10, 12]. Not only does this serve as a cellularly derived primer, but it inhibits cellular translation and protein synthesis. This in turn will limit intracellular antiviral responses to the infection.

The viral mRNA is translated by cellular ribosomes to create viral proteins. Viral proteins used for transcription and replication, such as PB1, PB2, and PA, are rapidly transferred back into the nucleus [10]. Viral membrane proteins, such as HA, NA, and M2, are transported to the cellular membrane to create viral protein agglomerates within the membrane to prepare for packaging and budding [10].

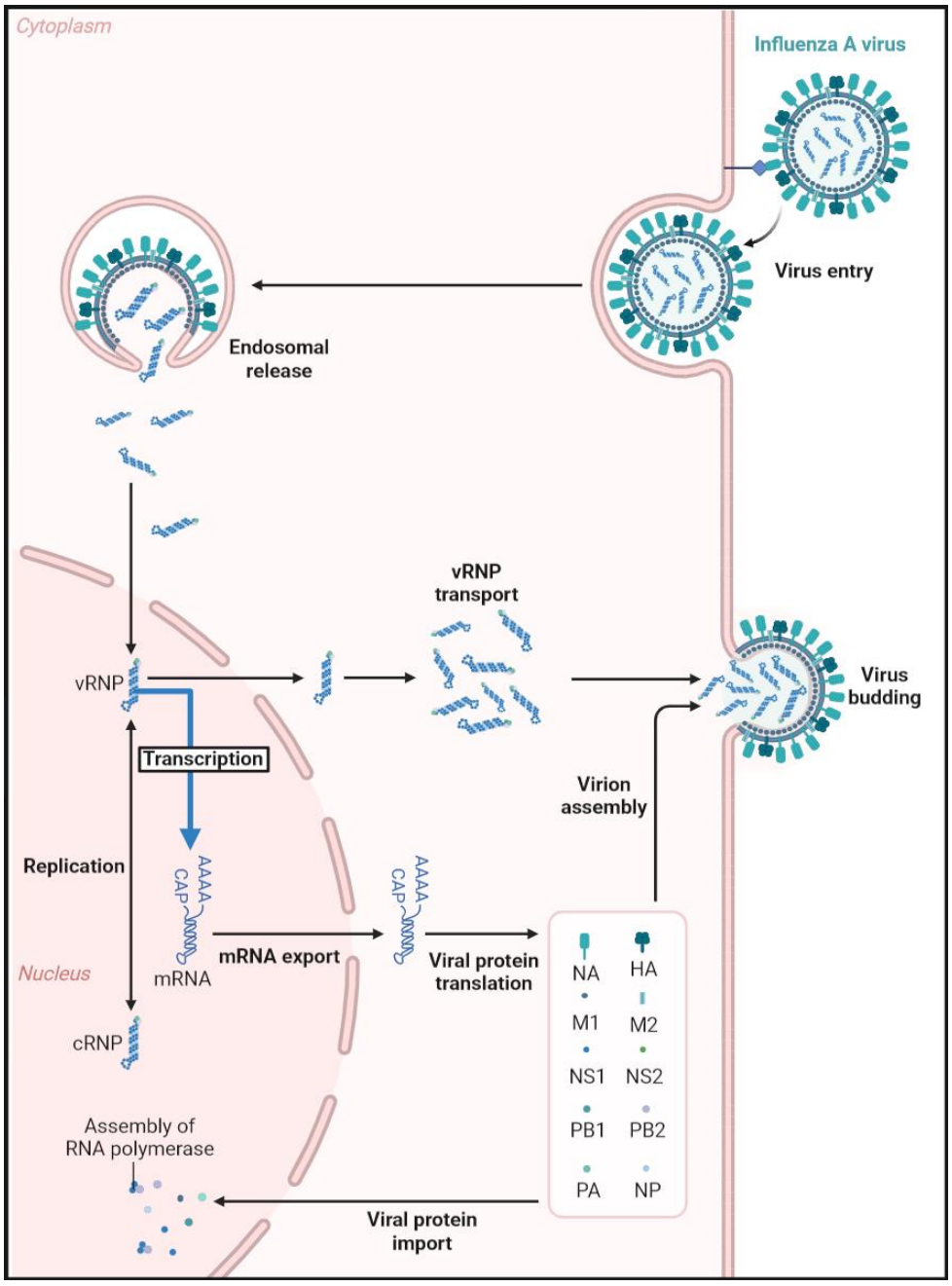

Figure 1.2: Influenza A Virus Replication Cycle: *Influenza A viral replication first begins with binding of cell surface sialic acids by the Hemagglutinin. Following endocytosis, the acidification of endosome leads to membrane fusion and release of vRNPs into the cytoplasm. The vRNPs then localize to the nucleus where they begin transcription and replication, leading to the production of mRNA and complementary RNP (cRNP). Viral mRNA is then translated into proteins, which either localize back to the nucleus, or begin assembly of the virion. cRNP is then used as a template to generate vRNP, which are then exported for virus budding [7-9].*

Before viral replication can begin, a positive sense intermediate must first be constructed. These cRNP or complementary ribonucleoprotein complexes are used as a template for the replication of negative sense vRNA genome segments. Unlike transcription, there is no evidence that genome replication requires an external primer [12]. Towards the later stages of viral infection, several viral proteins including M1 and NEP, nuclear export protein, will localize to the nucleus and facilitate the export of vRNP into the cytoplasm [10]. These complexes will then migrate to parts of the cellular membrane containing HA, NA, and M2, and are consequently bundled up and bud off into new virions. The NA ensures a successful exit by preventing accidental rebinding of mature virions to the host cell by cleaving the sialic acid receptors [10].

CROSS SPECIES TRANSMISSION TO DOGS

Interspecies transmission is a cornerstone of viral evolution. It allows a virus to expand beyond its original host reservoir. In the case of Influenza A, this typically occurs by two means [15]. The first is direct, unaltered transmission of the virus from one species to another. This transmission event often relies on antigenic drift and relative similarity

between hosts in order to sustain itself within a new population. Antigenic drift is categorized as the random mutations/nucleic acid substitutions that occur naturally during genome replication [11]. Often these mutations aid in avoiding immune responses by changing important antigenic components of the virus [13]. In the case of influenza, these components are Hemagglutinin (HA) and Neuraminidase (NA), and altering them allows the virus to maintain circulation within a population despite established immune responses [11]. These mutating viruses must maintain the fine line between avoiding immunity without losing functionality of their proteins. The other mechanism is antigenic shift or genetic reassortment [11, 15]. Genetic reassortment is a result of a particular quality of influenza itself, its segmented genome. During co-infection with two different strains of influenza, genome segments can get mismatched, resulting in the generation of a novel virion with a mixed set of genome segments [11, 15]. Oftentimes, this results in a dud, dead end infection, however, the right combination of segments and environmental factors can result in rapid spread or even infection into a new host population. Evidence supports this as three out of four influenza pandemics, the 1957, 1968, and 2009 pandemics, all have strong indications they originated from genetic reassortment [15].

An excellent example of interspecies transmission was in 2004, when 22 racing greyhounds from Florida fell ill with a respiratory illness [15]. Some outcomes were relatively mild, with dogs contracting a cough and fever, before recovering. Eight dogs unfortunately suffered a much crueler fate, hemorrhaging in the respiratory tract before death. This outbreak had a shocking fatality rate of 36%, as eight of the 22 dogs suffered from fatal cases [15]. Thankfully, as it spread through the US, the fatality rate dropped as the number of cases increased [15]. Until then, dogs were considered impervious to

influenza virus infection, based on the absence of documented outbreaks in this species. This perspective was drastically altered as Crawford et al. unveiled that an H3N8 influenza A virus was responsible for this epidemic.[15]. Phylogenetic analysis performed by Crawford et al showed it was closely related to H3N8 equine influenza as it had more than 96% sequence identity with equine influenza [15]. Due to the close proximity these greyhound dogs had to horses, it is likely that these dogs' acquired influenza from infected horses.

This is not the end of the story for Canine Influenza virus (CIV). In Korea, from May to September 2007, another severe respiratory illness was spreading rapidly in dogs [16]. This disease resulted in very similar symptoms to the previous outbreak in 2004: coughing, fever, nasal discharge, and even death. A total of three strains were isolated and all were identified to be influenza [16]. With all eight gene segments sequenced, phylogenetic analysis discovered this outbreak was not caused by the same H3N8 virus, but a novel influenza virus that was 95.5-98.9% identical with H3N2 Avian Influenza A virus isolates [16]. A new H3N2 subtype of CIV was identified.

SPREAD AND PREVALENCE OF CIV IN DOGS

H3N8

After its emergence in dogs in Florida, H3N8 CIV quickly spread throughout the US. Considering that there had been no previously identified influenza viruses in canines, most dogs were immunologically naïve, allowing the virus to spread first to Texas, then Iowa and New York, before eventually being identified in 38 total states by 2010 [17-19]. This spread was not reproduced outside the US. While there were cases of possible

detection later, H3N8 never became established within dog populations [18, 20]. Locations with high or dense dog populations have the most risk for endemic or enzootic CIV [21-23]. Dog shelters in Colorado and New York frequently exhibit a high prevalence rate, with certain shelters reporting a seropositivity rate as high as 10% [21]. Dog shelters or daycares are often the areas that pose the highest risk for infection and act as hotspots, as dog populations present at these locations have higher seropositivity for CIV than household dogs [23, 24]. The major CIV outbreaks in Colorado and New York died down in 2012 and 2016 respectively, with little to no disease being detected since [17]. Despite the rapid spread of H3N8 during the first decade of its emergence, its seroprevalence now is usually low and patchy, only existing within small, isolated dog populations [23]. The limited contact between dog populations may be the driving factor for the slow fade out of H3N8 CIV [22].

H3N2

The H3N2 subtype of CIV was first identified in Korea [17]. Archived serological samples from dogs show that infection could have potentially been present as early as 2005 [25]. Estimations, based on the rate of CIV evolution, place the origin of CIV earlier, between the years 2002 and 2004 [26]. Initial analysis indicated the origin was a single crossover event from avian sources, however it wasn't until 2015 that a more complex origin was suggested. After performing phylogenetic analysis of the genome, Zhu et al. discovered that several of the genome segments clustered separately from the others, with distinct phylogenetic relationships [27]. This hints at a more complex origin to this virus than originally thought, potentially resulting from an intricate reassortment of a variety of avian IAVs.

Similar to H3N8, the H3N2 subtype rapidly spread throughout Korea and the rest of Asia [28, 29]. The current state of dog populations in Asia provides a perfect environment for CIV, as large populations of stray dogs, farm raised meat dogs, as well as pet dogs cater towards maintained and endemic CIV circulation within South Korea and multiple providences in China [30]. The seroprevalence of the H3N2 subtype throughout Asia ranges quite drastically, from 1-33% across different pet dog populations [20, 29, 31-36] CIV infection appears to be much higher in stray dogs, with a separate study reporting populations with a prevalence as high as 48% [36]. It appears that the prevalence is on an upward trend as the seropositivity for CIV at the Veterinary Teaching Hospital of China Agricultural University in Beijing had risen from 3.5% in 2013 to 6.3% in 2017 [32, 33]. This is corroborated by a serological survey performed from 2016-2018, as the percent of samples positive for H3N2 went from 6.68% in 2017 to 18.89% in 2018 [36].

In February 2015, CIV H3N2 infections were initially detected in Chicago and rapidly spread through animal shelters, boarding kennels, and veterinary clinics throughout North America [37]. Whole genome sequencing suggested it originated from South Korea. By May of that year, it had already become widespread, reaching western and eastern states, including California, Georgia, and Pennsylvania [37]. H3N2 CIV quickly spread through these dog kennel and shelter populations, but the minimal contact between pet dogs limited further spread, leading H3N2 to a very similar fade out fate to H3N8 in the US [23, 37]. Despite this, outbreaks continue to occur in the US, often being tied to reintroductions from Asia [23, 38]. The limited contact in the US between pet dog populations is not favorable for CIV maintenance, therefore, the pop-up epidemics that are fueled by these reintroductions of H3N2 CIV from Asia, fade out within a year [23,

38]. At present, the seroprevalence of H3N2 CIV in North America is comparatively low, reaching only around 3-5%. However, this does not diminish the seriousness of the threat as there have been several CIV outbreaks caused by reintroductions from Asia. [23, 38, 39]. The low seroprevalence could also indicate North American dog populations are generally more immunologically naïve to influenza, leading them to be more susceptible to outbreaks.

DOGS AS A MIXING VESSEL

Mixing vessels is the term coined for host species where reassortment is common [30, 40]. This is often due to the susceptibility to multiple strains of influenza virus. The primary example of a mixing vessel is pigs. Due to the presence of alpha-2,3 and alpha 2,6 sialic acids throughout the respiratory tract, pigs are potentially susceptible to influenza from both avian and mammalian sources [41]. Therefore, the respiratory tract of pigs serves as the perfect environment for co-infection and reassortment of both avian and mammalian influenza [40]. Dogs, recently added to the list of influenza hosts, may also play a role as a mixing vessel for influenza. With both alpha-2,3 and alpha 2,6 sialic acid receptors having been identified in the upper respiratory tract of dogs, they additionally have the potential to be susceptible to a large variety of influenza strains [30, 41]. Studies have shown the susceptibility of dogs to human pandemic09 H1N1, and avian H6N1, H5N1, H9N2, and H5N2 strains which supports the potential for co-infection and reassortment [42-48]. Multiple Influenza reassortments have already been isolated from dogs, including several reassortments between swine and canine strains, a H3N1 reassortment between pandemic09 H1N1 and H3N2 CIV, and a relatively recent H3N6 reassortment between H5N6 AIV and H3N2 CIV [42-48]. The most threatening

part of H3N6 was that it was isolated from several dogs within the same shelter, indicating it had the potential to spread, but fortunately it was minimal [42]. With the proximity that dogs have to humans as companion animals, the potential threat of emergent pandemic strains through zoonotic transmission and reassortment remains extraordinarily high.

CHAPTER 2: CIV MOSAIC IMMUNOGEN DESIGN

INTRODUCTION

Influenza Vaccines and History

Vaccines for influenza virus have almost as long of a history as the discovery of influenza itself. With the discovery of the virus occurring in the 1933, the first vaccine was developed only a decade later [49, 50]. A couple years later, it was discovered that this vaccine was ineffective at protecting against the newly circulating flu viruses [49]. This lack of effectiveness can be attributed to multiple reasons. First, there are many influenza strains that can potentially circulate, due to the various HA and NA combinations. This has led to the development of many surveillance systems with the goal of identifying and predicting influenza strains with the highest probability of circulating in the upcoming season [3]. Therefore, influenza vaccines are based on these predictions each year [3, 49]. Unfortunately, the predictions do not always match the circulating strain, leaving vaccine efficacy to be very spotty over the years. The average effectiveness for influenza vaccines is around 38%, reaching as high as 60% in years where the vaccine matches the circulating strain, and as low as 10% in unmatched years [51]. Constructing trivalent or quadrivalent vaccine cocktails attempts to remedy this, but vaccine effectiveness is still variable and often nowhere near desired levels [3, 7]. Next, antigenic drift can allow viruses to mutate and slowly drift away from chosen vaccine strains, allowing for the generation of immune escape variants [13, 51]. Finally, genetic reassortment and cross-species transmission can introduce novel influenza viruses into populations that have no previous exposure [5, 51]. These events are almost entirely random and unpredictable, with the best currently available protective measure being

prevention. Proof of the threat this poses is the 2009 Influenza pandemic that resulted from a triple reassortment in pigs, which completely took over as the dominant circulating strain of influenza for the season and future seasons to come [5].

Types of Influenza Vaccines

Egg-based inactivated influenza vaccines are the most dominant and cheapest method of vaccine production. The large production capacity of roughly 1.5 billion doses a year along with the low-cost relative to other methods has kept egg-based vaccines at a high market share of 88% as of 2018 [7, 51]. However, this is not without its drawbacks. Since manufacturing takes anywhere from 6-8 months, vaccine strains must be selected well before the flu season [7, 51, 52]. Antigenic drift can quickly cause circulating strains to no longer match vaccine strains, therefore, the larger the period of time between vaccine strain selection and administration, the higher the probability it will be ineffective. While being cultured in eggs, the high mutation rates of influenza also threaten the integrity of vaccine virus strains as they adapt to avian tissue [7]. The half year or more production time limits responsiveness to delays in strain selection, pop up pandemic variants of influenza, or low virus yields, and it is heavily limited by egg supply [7].

Live attenuated influenza vaccines are based on cold-adapted strains of influenza. Reassortant vaccine viruses are generated by swapping the HA and NA of cold-adapted influenza viruses, with that of currently circulating strains [7, 52]. This produces a virus that has limited replication ability in the respiratory tract and is administered intranasally. The major benefits of this method are that it appears to generate mucosal immunity and a strong cell mediated response [7, 51]. However, these are often grown through egg-based methods as well and are dependent on the ability to replicate in the respiratory tract [7,

51]. Also due to the attenuation rather than inactivation of these vaccines, genetic reassortment with circulating influenza remains possible.

In an attempt to remedy the issues with egg-based vaccines, cell-based manufacturing processes have been developed [51, 52]. The growth of viruses in cell culture allows for more flexibility and is unaffected by egg shortages. However, the cost is often higher than egg-based production, which has limited its share in the market [7, 51].

Vaccine Immunology

Influenza vaccines and aim to generate an adaptive immune response. The immune system can be divided into two major subclasses, the innate immune system, and the adaptive immune system [53]. The innate immune system is germline encoded and is typically the first line of defense against pathogens. The innate immune system is generally considered non-specific and has limited memory, as it responds to all pathogens in a similar manner after recognizing conserved pathogen-associated molecular patterns (PAMPs) or damage-associated molecular patterns (DAMPS) [53-55]. Adaptive immunity is much more specific and is further divided into humoral and cellular immunity [4]. Humoral immunity is mainly facilitated by B lymphocytes which are responsible for generating antibodies [4, 53]. Cellular mediated immunity (CMI) is facilitated by T lymphocytes which are responsible for assisting and activating immune components, along with identifying and eliminating infected cells [4, 53, 55]. By utilizing these B and T lymphocytes, the adaptive immune system can recognize specific molecular patterns from a pathogen [53]. Typically, the adaptive immune system must be primed in order to achieve the most efficient immune response, as it relies on its ability to generate long term memory for pathogens [55]. Therefore, during the initial response to a

pathogen the adaptive immune response is slow, however subsequent exposures to the same intruder initiate quicker and more specific adaptive immune responses [53]. The goal of vaccines is to utilize this quicker response by priming the adaptive immune system through exposure to pathogenic molecules. Consequently, memory can be generated without natural infection, leading to efficient responses during a future encounter with the pathogen. In regards to influenza, inactivated influenza vaccines mainly induce strong antibody responses [4]. These antibodies tend to be very strain specific, limiting their ability to protect against mismatched strains [4]. To combat this, there has been a push for influenza vaccination strategies that target the more broadly protective cellular mediated immunity [4].

CIV Vaccines

The current commercially available CIV vaccines are a monovalent or bivalent cocktail of inactivated influenza viruses. Zoetis and Nobivac are front runners for these vaccines, but there is a huge drawback. The vaccine strains used are at least 8 years outdated [56, 57]. Zoetis' vaccine, Vanguard, utilizes a bivalent CIV cocktail of an inactivated H3N2 from 2015, and a H3N8 from 2005 [56]. Nobivac is not much better, since their vaccine contains an inactivated H3N2 from 2015 and a H3N8 from 2006 [57]. As previously discussed, due to the high mutagenicity and variability of circulating influenza strains, influenza vaccines must be updated annually to ensure the highest possible effectiveness. Despite having an overall slower mutation rate and less availability of hosts for CIV, this does not justify the outdated vaccine strains [27]. There is evidence to suggest that these vaccines exhibit suboptimal levels of efficacy, as demonstrated by a CIV outbreak in

Canada wherein 60% of the infected canines had previously received vaccinations [38, 58].

Major Influenza Immunogen

Hemagglutinin (HA) is a homotrimer that exists on the surface of influenza particles. HA is the most abundant protein on the surface of influenza viruses, often outnumbering neuraminidase 5 to 10-fold [10, 13]. Due to this abundance, HA is a common immune target and considered the major antigen of influenza virus, leading to influenza vaccines requiring 15 ug of HA per vaccine strain for each dose [13] [59]. The large globular head, contained mostly within the HA1 subunit, houses the receptor binding domain (RBD) and has the majority of antigenic sites, or regions targeted by the humoral immune response [10, 13]. The stem, within the HA2, is less immunogenic, eliciting a lower antibody response [13]. Most of the antibodies generated against the globular head are strain specific. This is due to antigenic drift as the antigenic sites within the globular head exhibit the highest detected amino acid mutation rates because it subverts herd immunity [13]. Because the RBD, located within the globular head, is essential for viral infection, these mutating viruses must maintain the fine line between avoiding immunity without losing functionality [13].

For the majority of IAV history, antibodies have been used as the indicator of protection. The hemagglutination inhibition assay has been a staple within the IAV field to quantify the level of protective antibodies within serum [60]. This assay attempts to measure HA inhibiting antibodies by determining the highest dilution of sera that can prevent red blood cell agglutination [13, 60]. While antibodies can be good correlate of protection, vaccine induced antibodies are strain-specific which limits protection against mismatched

strains [4]. Cell-mediated immune (CMI) responses through recent years have also been shown to be a correlate of protection, with the added benefit of generally being more cross-reactive against various IAV subtypes [4]. Therefore, due to the high abundance of hemagglutinin on influenza's surface and the general cross-reactivity of CMI, we developed a computational HA immunogen through the Mosaic Vaccine Designer that attempts to maximize T cell responses to our immunogen [61].

Mosaic Immunogen Design

The Mosaic Vaccine Designer was originally designed by the Los Alamos National Laboratory for HIV immunogen development [61]. HIV vaccine development suffers from similar issues as influenza vaccine development. The extreme diversity of HIV-1 along with high mutagenicity has prevented the development of a universal vaccine [61]. Therefore, a computational algorithm was developed that attempts to maximize theoretical T cell epitope coverage by creating a mosaic immunogen from a set of natural sequences [61]. The mosaic immunogen resembles natural proteins, with the algorithm incorporating common amino acid 9-mers from the natural sequence population, while excluding rare 9-mers [61]. These 9-mers serve as potential T cell epitopes as CD8+ T cells recognize 8 to 10 amino acid length peptides presented on major histocompatibility complexes (MHC). Theses peptides originate from endogenous proteins and if an infected cell presents a viral peptide, CD8+ T cells can recognize and induce apoptosis of the infected cell [4]. Thus, these mosaic immunogens include common potential T cell epitopes in attempt maximize broadly protective cellular immune responses [61].

The Mosaic Algorithm begins with a population of natural sequences. and through random two-point recombination, a set of recombinant sequences are generated.

Recombinants are eliminated if they contain unnatural or rare 9-mer epitopes. The most "fit" sequence is selected from the recombinant population as the representative. Fitness is determined by evaluating the coverage of natural 9-mers sequences contained from the natural sequence population, the higher the coverage, the higher the fitness. Sequences are further optimized by selecting four recombinant sequences (parent sequences) at random and evaluating their fitness. The two with the highest fitness then undergo two-point recombination and generate a new recombinant. This new sequence has the potential to replace the originally selected representative if it has a higher diversity of natural epitopes. If it does not have a higher diversity than the representative, but it has higher fitness than one of four randomly selected parent sequences, it replaces that sequence. This is optimization is repeated until there is no improvement in fitness (Figure 2.1) [61].

The major benefit in utilizing a mosaic immunogen, rather than updating current vaccines with new strains, is that the mosaic immunogens are intentionally biased towards T cell responses [61]. Inactivated influenza vaccines (IIV), such as the ones currently available for CIV, tend to elicit very strong, strain specific humoral responses, but inefficient CD8+ T cell responses [4]. Consequently, as cell mediated immunity is generally more cross-protective against influenza than humoral immunity, IIVs provide poor protection to mismatched strains [4]. However, a mosaic immunogen biased toward cellular immune responses is theorized to induce more universal protection. Some studies have demonstrated the potential of mosaic vaccine approach to induce broad protection for the antigenically diverse influenza. Vaccination with a H5 Mosaic induced broad humoral and cellular responses and protection in mice [62]. Our lab has developed a Mosaic H1

vaccine vectored by human Adenovirus type 5 (HAd5) that was able to induce broad protection in mice as well [63, 64]. However, no attempt has been made to apply this to CIV vaccine development. Our lab hopes to develop a mosaic CIV HA that will provide broad protection in dogs.

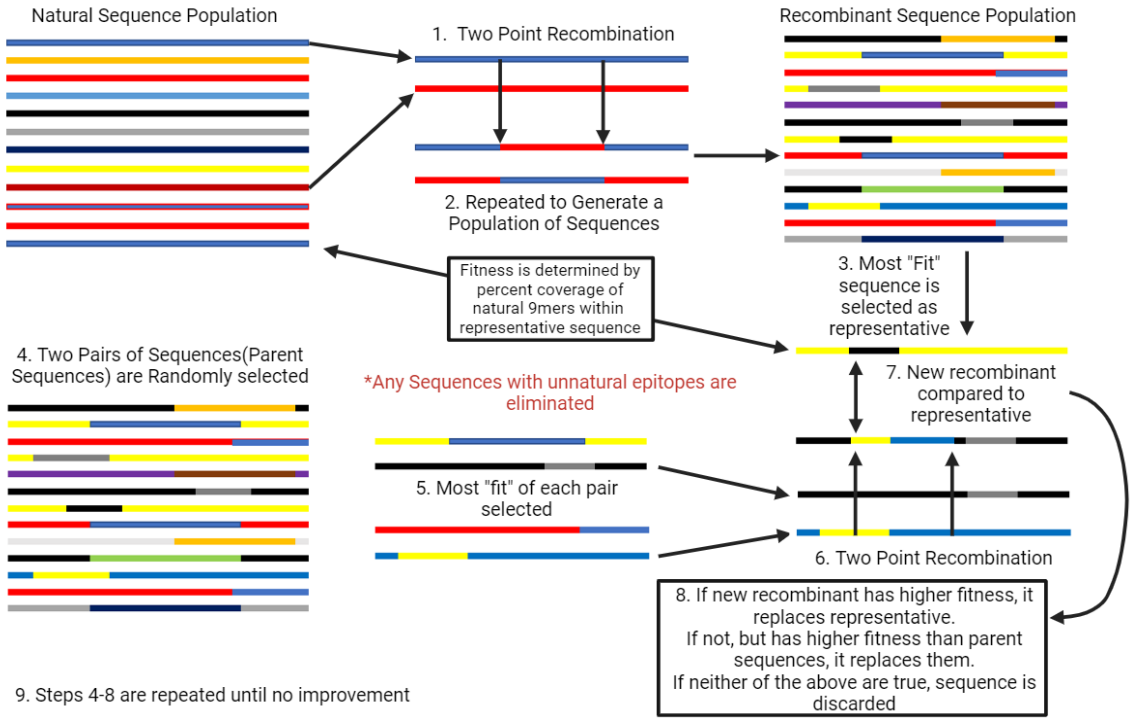

Figure 2.1: Mosaic Immunogen Designer Algorithm Workflow: *A schematic adapted from Fischer et al. 2007. (1) The Mosaic vaccine designer begins with a natural set of protein sequences. Two sequences are randomly selected for two-point recombination. (2) This is repeated until a new population of recombinant sequences are generated. (3) The most "fit" sequence is selected as the representative. Fitness is determined by the percent coverage of natural 9mers within the population representative. (4) Further optimization is performed by selecting two random pairs (parent sequences) from the recombinant population. (5,6) The most "fit" from each pair is selected for two-point*

recombination. (7) The new recombinant is compared to the current population representative. (8) If the new recombinant has higher fitness, then it replaces the representative. If not, but instead has higher fitness than either parent sequence, it replaces them. If neither are true, then it is discarded. (9) Steps 4-8 are repeated until there are no improvements.

RESULTS

Generating Canine Hemagglutinin (CanH3) Mosaic

All 156 available CIV Hemagglutinin sequences up until June 6th, 2022, were downloaded from the Influenza Research database. All duplicate and laboratory strains were excluded to minimize skewing towards overreported influenza strains and maximize coverage for naturally circulating strains. The resulting sequences were aligned using ClustalW and then uploaded to the Los Alamos Laboratories Mosaic Vaccine Designer. A single Mosaic CIV HA (CanH3 Mosaic) sequence was generated. The Mosaic Vaccine designer picks a mosaic sequenced based on the relative fitness or the number of theoretical T cell epitopes (9-mers) within a single sequence. Therefore, along with the Mosaic sequence, the output includes data encompassing the relative "fitness" of the chosen sequence (Figure 2.2). Fitness is based off the average percentage of each input sequence's 9-mers that are present within the mosaic sequence, the higher the percentage, the higher the fitness [61]. The generated CanH3 Mosaic sequence has a mean coverage of approximately 82% of all natural 9-mers found in each sequence of the original uploaded population.

After generating the Mosaic CIV HA (CanH3) sequence, it was aligned will all other CIV HA sequences to develop a neighbor joining tree (Figure 2.2). The tree has two major clusters; an H3N8 cluster denoted by red and an H3N2 cluster denoted by blue. The relative position of the Mosaic CanH3 is marked, and it localizes centrally in the H3N2 cluster. The large skew towards H3N2 can most likely be attributed to the much larger pool of publicly available CIV H3N2 sequences when compared to H3N8, as only 16 H3N8 sequences have been reported as of 2022. This can potentially create worry that the Mosaic CanH3 vaccine won't be able to protect against H3N8 strains of influenza. However, clustering within H3N2 sequences is currently more preferrable as H3N2 is accountable for most CIV infections [17, 21, 23, 24]. H3N8 has not been reported since 2016 leading to a much higher priority for protection against H3N2 strains [17].

The CanH3 Mosaic sequence, approximately 1700 nucleotides long, was ordered in the form of a pFastBacI vector (Figure 2.3a). Utilizing GeneArt Instant Designer, the sequence was uploaded, codon-optimized, and a 6x his tag was inserted at the 3' end. For future restriction digest, NotI and HindIII cloning sites were added, flanking the 5' and 3' sites respectively. Not I and HindIII restriction sites were chosen because they are not present within our CanH3 Mosaic sequence. The resulting sequence was optimized to protect NotI and HindIII restriction sites and avoid PacI and PmeI sites. PacI and PmeI were avoided since they are essential for future cloning. In order to confirm the presence of the transgene, pFastBacI was NotI and HindIII digested and run on a 0.8% agarose gel (Figure 2.3b). Two bands are shown on the gel, one at 4.2 kb and the second at 1.7 kb, which is approximately the size of the CanH3 Mosaic insert. This provides confirmation of the presence of the insert, within pFastBacI.

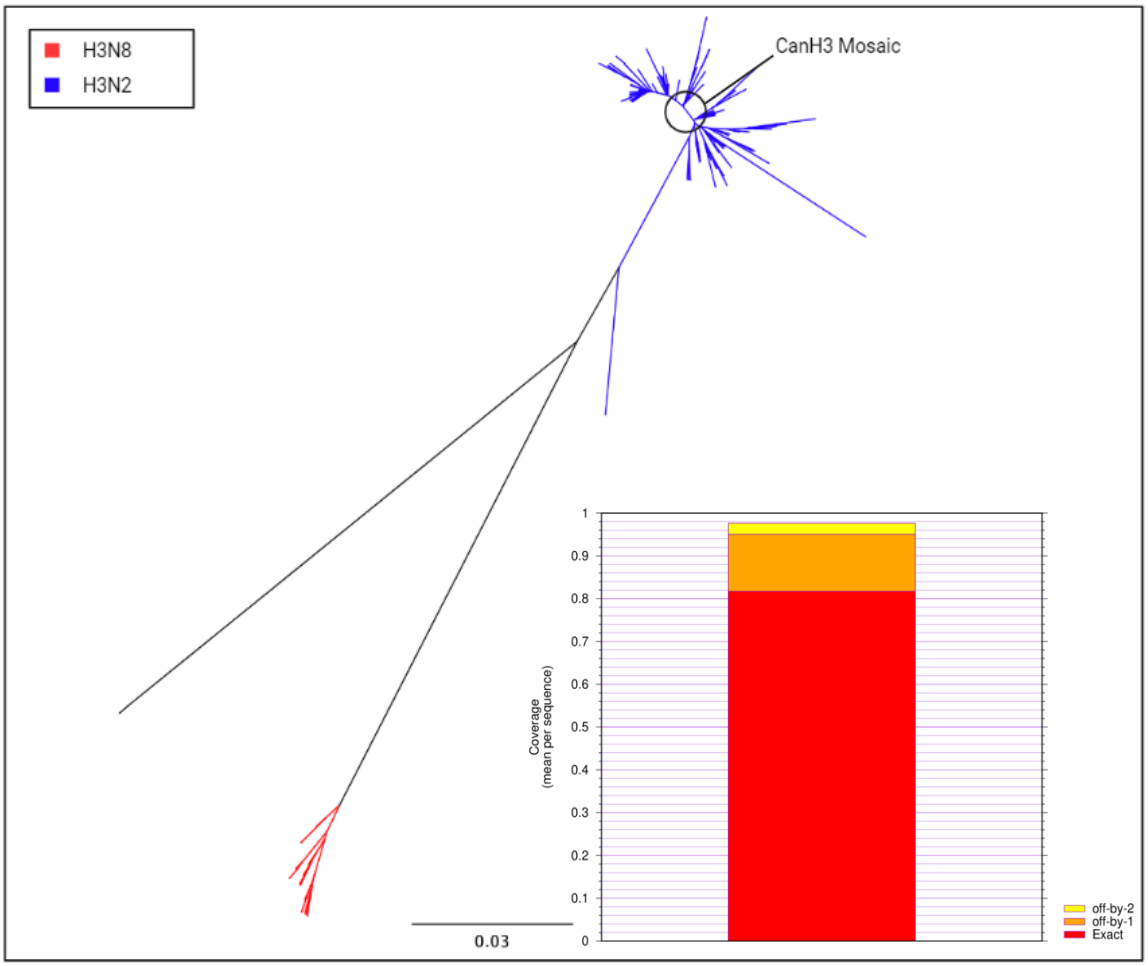

Figure 2.2: Phylogenetics of CIV HA sequences and CanH3 Mosaic.

(A) A Phylogenetic tree generated using all 156 publicly available natural CanH3 sequences, including the Mosaic CanH3 developed in Silico. Red denotes H3N8 sequences, while blue denotes H3N2 sequences. The relative location of the CanH3 Mosaic is marked and localizes centrally in the H3N2 cluster. (B) A graph depicting the mean percent coverage the CanH3 mosaic sequence has of all natural 9-mers within each input sequence from the original population. It depicts around 82% coverage.

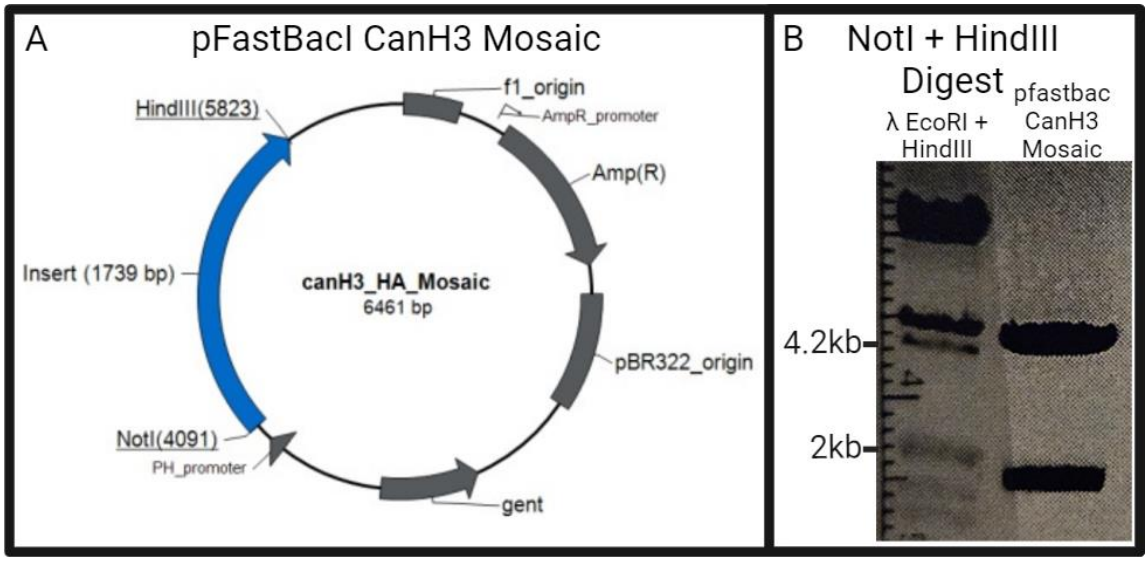

Figure 2.3: pFastBacI CanH3 plasmid map and restriction digest: *(A) A schematic showing the plasmid map for the pFastBacI with CanH3 Mosaic ordered from GeneArt. NotI and HindIII flank the approximately 1700 bp gene on the 5' and 3' ends respectively. (B) pFastBacI CanH3 Mosaic was digested with NotI and HindIII to confirm presence of insert. Two bands are shown, one just above 4.2 kb and one around 1.7 kb, with the latter having the expected size of the transgene insert.*

DISCUSSION

Development of a broadly-protective influenza vaccine has been a goal that vaccinologists have been seeking for decades. Due to the vast amount of circulating influenza strains, along with its high mutagenicity, most times a new vaccine is developed, the strains used are mismatched within a year [3]. Because a majority of the antibodies produced by current vaccines are strain-specific, they are ineffective against new strains. The high antigenicity of the rapidly evolving globular head prevents the long-term effectiveness of these antibodies [3, 4]. Therein lies one of the biggest challenges in developing a universal influenza vaccine. Canine Influenza Virus is not free

of these issues, as currently available CIV vaccines use outdated strains and potentially have limited effectiveness. With the ever-looming risk of zoonotic transmission and the dog's potential capacity to be the next pandemic producing mixing vessel, an effective vaccine is warranted.

In this chapter, we attempted to remedy this by developing a computational HA immunogen that maximizes potential T cell epitopes from all naturally available sequences, in one single immunogen. T cells play an essential role in antiviral immunity and may play a larger part in providing broadly protective immunity to Influenza A virus [4]. Specifically, CD8+ T cells play a key role in influenza virus immunity as they detect and eliminate infected cells, release cytokines important for the antiviral immune response, and reduce the severity of disease. Since inactivated influenza vaccines are inefficient at inducing CD8+ T cell responses, we therefore chose to use the mosaic computational algorithm to maximize potential 9-mer epitopes within our immunogen sequence to enhance the CD8+ T cell response [4].

After developing the Mosaic Immunogen, phylogenetic analysis showed it had a very central localization within the H3N2 HA sequences (Figure 2.2). As H3N2 appears to be the predominant CIV subtype, this is theoretically the ideal outcome, as our immunogen will have the most similarity to currently circulating strains [17]. If H3N8 does resurge however, our CanH3 Mosaic immunogen's potential effectiveness could drop. The central localization of CanH3 mosaic within the H3N2 cluster has the added benefit of being equally distant to most of these strains, potentially maximizing coverage. One main drawback could have been a high average divergence between our CanH3 mosaic and the H3N2 HA sequences, leading to a drop in effectiveness. We note that our mosaic does

not have any divergence greater than 5% to any of the available H3N2 HA sequences, so we theorize this is a minor issue. Our mosaic covers on average 82% of all reported natural 9-mer epitopes within an input natural sequence, which demonstrates confidence in its ability to induce broad protection. However, this can only be tested once the vaccine is fully developed through immune correlates and challenge studies.

Another potential limitation of this immunogen is that it is developed from only 156 available sequences. Comparatively there are thousands of available sequences for other influenza viruses that infect pigs, humans, and birds. This could be due to a general lack of surveillance for CIV, and it is impossible to theorize how well our vaccine could work against undocumented strains. Ideally, the relatively low number of sequences could be due to CIV's shorter history or simply being a less common infection. However, as the majority of CIV circulation occurs within Asia, there would have to be increased surveillance to get an improved grasp on which, if any, of these hypotheses are true.

Finally, we ordered in vitro synthesis of our mosaic immunogen, in a pFastBacI plasmid backbone. We confirmed functionality of the potential HindIII and NotI sites flanking our immunogen through restriction digest. Therefore, our immunogen has the capability to be cloned in future endeavors. In future chapters, we plan to further this study by cloning our gene into both human Adenovirus Type 5 and Canine Adenovirus Type 2 vectors, to test the efficacy of our mosaic immunogen.

METHODS

Mosaic CanH3 Development

All publicly available CIV HA sequences were downloaded from the Influenza Research Database (fludb.org). On the influenza research database, all HA protein sequences isolated from dog hosts were searched for using the following parameters: Data Type: protein, Virus Type: A, Classical Proteins: HA, HA subtype: H3, Host: Dog. To further refine the search, under advanced options, we selected exclude laboratory strains and remove duplicate sequences. A total of 156 sequences were found and then downloaded as a FASTA protein file. The file was uploaded to Geneious Bioinformatics Software to perform a ClustalW alignment using the following parameters: Matrix cost: BLOSUM, Gap open cost: 10, Gap extended cost: 0.1. Sequences were once again exported as a FASTA protein file. All sequences were uploaded to the Mosaic Vaccine Designer (https://www.hiv.lanl.gov/content/sequence/MOSAIC/makeVaccine.html) and the program was run with the following parameters: Cocktail size: 1, Run time:10 hours, Stall time: 10 minutes, Epitope Length: 9, Population Size: 200, Internal crossover possibility: 0.5, Rare Threshold: 1, Cycle time: 10. The resulting CanH3 Mosaic sequence was then exported for further use.

CanH3 Mosaic Phylogenetic Analysis

The CanH3 Mosaic was uploaded to Geneious bioinformatics software and input with all 156 CIV HA sequences. Sequences were once again aligned using ClustalW alignment with the following parameters: Matrix cost: BLOSUM, Gap open cost: 10, Gap extended cost. The aligned sequences were then used to generate a phylogenetic tree using the following parameters: Genetic distance model: Jukes-cantor, Tree building method: Neighbor Joining, Outgroup: no out group. The H3N2 and H3N8 CIV sequences in the resulting tree were colored blue and red respectively.

Ordering CanH3 Mosaic

CanH3 Mosaic Immunogen was ordered in the form of a plasmid through GeneArt Instant Designer (https://www.thermofisher.com/us/en/home/life-science/cloning/gene-synthesis/geneart-gene-synthesis.html). The CanH3 Mosaic sequences were uploaded into the GeneArt Instant Designer. Protein Sequence was selected as sequence type and canine was selected for host organism. pFastBacI was selected as the vector. The sequence was codon optimized and a 6x his tag and stop codon were manually inserted at the 3' end of the sequence. NotI and HindIII restriction sites were added to the 5' and 3' ends respectively by adding GCGGCCGCGCCACC to the 5' end and AAGCTT to the 3' end. Under the optimize tab, NotI and HindIII cloning sites were protected and PacI and PmeI were selected as motifs to avoid.

Restriction Digest of pFastBacI CanH3 Mosaic

Once pFastBacI CanH3 Mosaic was received, plasmid DNA was electroporated into XL-1 cells. 0.5μL of pFastBacI CanH3 Mosaic DNA was pipetted into 45 μL of XL-1 cells. 45 μL of ddH20 was added to cells before they were electroporated at 2500 volts for approximately 5 ms. Cells were then rescued in 350 μL of S.O.C. medium for 1 hours at 37 °C before being plated on LB + AMP plates and incubated overnight. Two single colonies were selected and grown in LB + AMP media overnight. Using a QIAprep spin miniprep kit (https://www.qiagen.com/us/products/discovery-and-translational-research/dna-rna-purification/dna-purification/plasmid-dna/qiaprep-spin-miniprep-kit) , plasmid DNA was isolated. 1 μg of plasmid DNA was then digested by 0.5 μL of NotI-HF and HindIII-HF at 20,000 U/mL(New England Biolabs) in a 20 μL reaction for 1

hours at 37 °C. Resulting digest was run on a 0.8% agarose gel at 30 volts for 30 minutes. Gel results were visualized using the Chemidoc using ethidium bromide imaging.

CHAPTER 3: INSERTION OF CANH3 MOSAIC INTO AN ADENOVIRUS TYPE 5 VECTOR

INTRODUCTION

Adenoviruses are icosahedral, nonenveloped viruses that belong to the *Adenoviridae* family. The viral capsid houses a linear, double-stranded DNA genome. The size of this genome can vary quite drastically, ranging from 25 to 48 kilobase pairs (kbps) depending on the Adenovirus subtype. Adenoviruses subtypes are species-specific and are known to infect a broad range of hosts, including birds, reptiles, amphibians, fish, and a variety of mammals including humans [65, 66]. The identified types of human adenovirus number over a hundred, and are classified into 7 species, labeled A to G. The subtypes are known to cause respiratory disease, gastroenteritis, or conjunctivitis [65]. Adenoviruses have been investigated extensively since their discovery, leading to a vast knowledge base regarding genome structure, viral lifecycle, and functions of viral genes [67, 68]. Viral genes can be divided into two classes, Early and Late, based on when they are expressed during the viral lifecycle. Early genes are often responsible for host immune and gene regulation, along with viral transcription and replication [65, 69]. Late genes, however, encode mainly structural proteins responsible for capsid formation and maturation of virions [65, 67, 69]. This extensive knowledge of gene location and function allows for relatively easy modification and manipulation to create safe, and highly efficient viral vaccine vectors [68].

One of the most common ways in which Adenoviruses are manipulated to become vectors is through Early 1 (E1) and Early 3 (E3) deletions. Within the E1 gene locus is an essential transcriptional activator, E1a. This E1a gene codes for one of the first proteins

expressed during adenovirus infection and is required for the expression of other viral genes [70]. Therefore, by replacing the E1 locus with a transgene, an adenovirus becomes replication-defective and able to induce high levels of transgene expression [65]. E3 deleted adenoviruses work similarly, but a transgene is inserted into the E3 locus. The E3 gene locus contains a variety of genes responsible for host immune regulation and is not essential for viral replication [67]. Deletion of the E3 locus can potentially enhance immunogenicity as many proteins responsible for immune evasion are removed. Both of these techniques are often combined to create E1/E3 deleted adenoviral vectors that are replication defective with enhanced immunogenicity [68].

Adenoviral genomes are easily cloned and manipulated using molecular biology techniques and, due to the viral component of these vectors, they serve as their own adjuvants [65]. These viral vectors can still initiate the first steps of viral replication, such as binding to cellular receptors, viral entry, and uncoating, before expressing the target antigen [68]. Mimicking a viral infection facilitates proinflammatory immune responses and activates various TLR-dependent and independent pathways by exposing the immune system to PAMPs [65, 68]. These properties allow Ad-vectored vaccines to elicit strong cellular and humoral responses against a target antigen [65, 66, 68, 71]. Beyond high immunogenicity, these vectors often have broad cellular tropism, providing the advantage of being delivered through multiple routes [65, 68]. With well described methods for vector development, and the ability to be grown in cell lines, adenovirus vectors are easily scalable for large production [65, 67].

Adenoviral vectors, however, aren't without their problems. One of the major issues of replication-defective Ads is that they require an E1 complementing cell line in order to

grow [66, 68]. This has been easily remedied by utilizing the HEK 293 E1 complementing cell line, but this introduces problems of its own. Production using this cell line can potentially generate replication competent adenovirus (RCA) because of homology between the vector and the E1 gene inserted into the HEK 293 cellular genome [68]. Cell lines with minimal homology have been developed to minimize this issue [68]. Preexisting immunity to viral vectors can also limit the effectiveness of these vaccines by neutralizing the vector, limiting transgene expression before an immune response can be mounted against it [65, 66, 68]. Vectors with low seroprevalence have been constructed in an attempt to subvert this, but they still suffer from the issue that vaccinating with these vectors induces an immune response against the vector itself [65]. Some studies suggest that a proper interval between vaccine doses of 6 months or more can give enough time for vector immunity to wane and adenovirus vectored vaccines to become effective again [65, 72]. Other methods such as changing vaccine route, coating the vector, and developing vectors with a chimeric hexon capsid protein have been tested and serve as promising alternatives to these problems [68].

Human Adenovirus Type 5 (HAd5) vectors are one of the most commonly used vectors in research studies [66]. Since HAd5 is often selected for research because of its high immunogenicity, methods for developing HAd5 vectors are some of the most well described and commercially available. He et al streamlined these methods by developing a series of plasmids that can easily be used to insert a specific transgene into HAd5 [67]. HAd5 vectors have the ability to infect canine cells and exhibit strong transgene expression [73-75]. Therefore, there have been a few applications of HAd5 vectors for dog vaccines, including recent use for Rabies virus, Canine distemper virus (CDV), and

Severe Fever with Thrombocytopenia Syndrome (SFTS) virus [73-75]. While replication defective HAd5 expressing CDV and SFTS immunogens have not been evaluated in dogs, they confer protective immunity in mice and foxes [73-75]. Another study by Vos et al. demonstrated intramuscular vaccination with a replication defective HAd5 vector expressing rabies G protein induced high levels of rabies virus neutralizing antibodies in dogs [76]. We plan to utilize an HAd5 vector for the delivery of our CanH3 mosaic immunogen. In this chapter, we demonstrate the steps we utilized to develop and confirm construction of a HAd5 vector containing our mosaic immunogen.

RESULTS

HAd5 CanH3 Vector Construction

To generate our recombinant HAd5 vector we used the AdEasy Adenoviral Vector System (Agilent). The system starts with cloning the desired transgene into pShuttle-CMV. This plasmid contains a multiple cloning site (MCS), flanked by a CMV promoter and polyadenylation site, along with areas of homology with HAd5 and a kanamycin resistance gene. It is mainly used to “Shuttle” a specific transgene into the genomic HAd5 plasmid through homologous recombination. We first NotI and HindIII digested our pFastBacI CanH3 and pShuttle-CMV to free our CanH3 mosaic immunogen and linearize pShuttle-CMV in the MCS. The CanH3 Mosaic was then ligated into the MCS through T4 ligation (Figure 3.1a). Confirmation for insertion of our transgene into pShuttle-CMV was performed by NotI and HindIII digesting the plasmids, before imaging the results on an agarose gel (Figure 3.1b). Our results show the formation of two bands on the gel, an approximately 7 kbps fragment which coincides with the

pShuttle-CMV backbone and a much smaller 1.7 kbp fragment the size of our expected transgene.

After confirming the construction of pShuttle-CMV with our CanH3 mosaic transgene, we proceeded with homologous recombination to insert it into the genomic HAd5 plasmid, pAdEasy. pAdEasy contains the majority of the HAd5 genome, with large portions of the E1 and E3 genes deleted [67]. Transgene insertion into the E1 locus is achieved through homologous recombination between pAdEasy and linearized pShuttle-CMV CanH3 within BJ5183 cells (Figure 3.2a). Successful recombinants were confirmed through PacI digest. The two PacI digest sites flanking the HAd5 genome are inserted during homologous recombination and should only be present if it was successful. PacI digest is expected to form two fragments, a 35 kbp fragment and a much smaller 3.5 kbp fragment (Figure 3.2b). Our results show very clear fragments at the expected sizes, supporting formation of our recombinant HAd5 plasmid. Further confirmation was performed through whole plasmid sequencing (Eurofins genomics). The sequencing results show an HAd5 genome that is mostly intact, except for the E1 and E3 genes, along with insertion of our transgene within the E1 region (Figure 3.2c). ClustalW alignment between the expected transgene insert (CanH3 Mosaic 1) and the sequenced transgene from this plasmid (CanH3 Mosaic Sequenced) showed 100% sequence identity, giving us further confidence that a successful recombinant had been constructed.

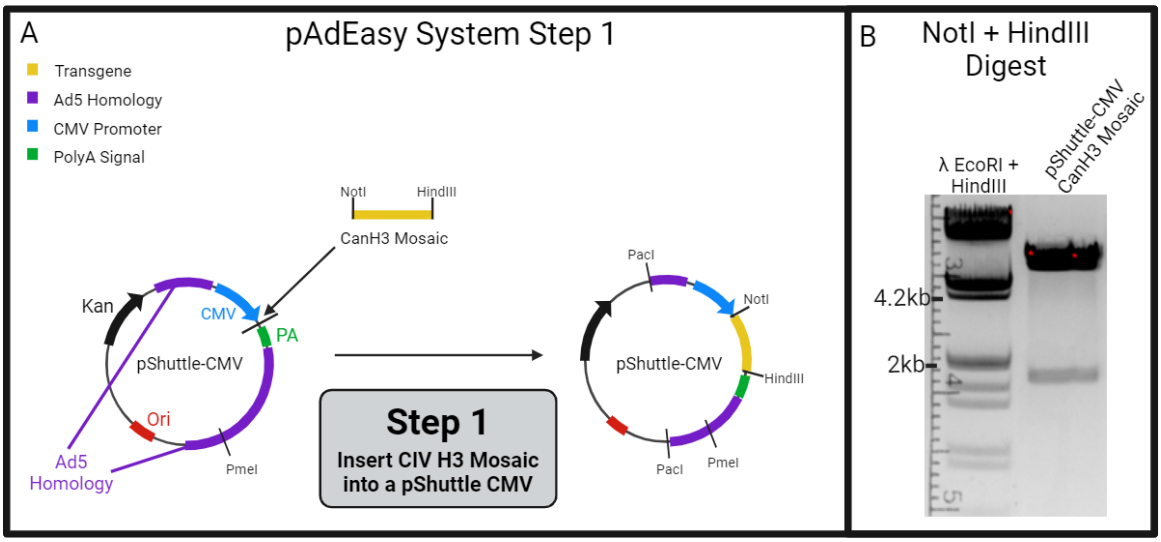

Figure 3.1: Insertion of CanH3 Mosaic into pShuttle-CMV: *(A) Schematic showing step 1 of the pAdEasy vector system. The CanH3 Mosaic gene is inserted into pShuttle-CMV through NotI and HindIII digest followed by T4 ligation. (B) pShuttle-CMV containing the CanH3 Mosaic was NotI and HindIII digested. Two bands form, the first around 7 kbps, corresponding to the pShuttle backbone, and the second around 1.7 kbps, corresponding to our transgene insert.*

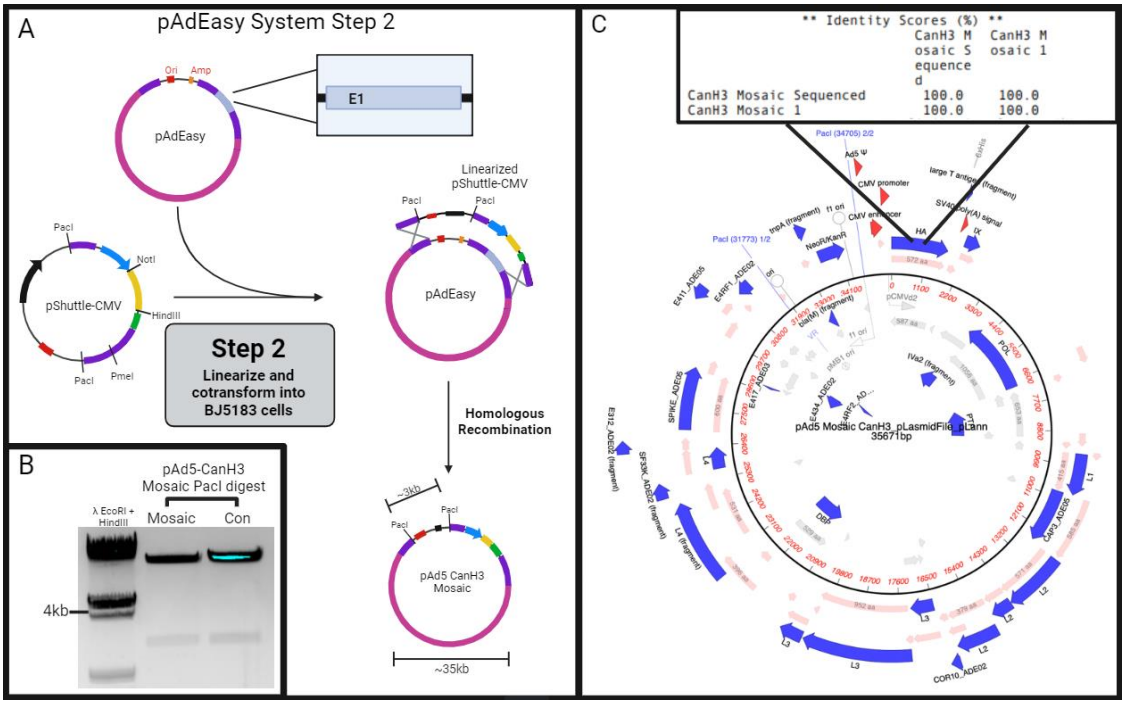

Figure 3.2: pAdEasy Vector System Step 2: *(A) Schematic showing the workflow for step 2 of the pAdEasy Vector System. pShuttle-CMV shuttles the transgene into the E1 region of the genomic HAd5 plasmid pAdEasy through homologous recombination in BJ5183 cells. (B) PacI digest to confirm homologous recombination and insertion into pAdEasy. The pair of PacI sites are not present unless recombination has occurred. Two fragments form on the gel, one around 3.5kbps with the other much larger. (c) Whole plasmid sequencing of a potential pAd5 CanH3. Sequencing confirmed the insertion of our CanH3 mosaic into pAdEasy. After aligning the transgene, it was confirmed to be 100% identical to the expected transgene.*

To confirm whether this recombinant HAd5-CanH3 Mosaic genome could produce virus, we transfected it into the E1 complementing cell line, HEK293 (Figure 3.3). We began by linearizing the HAd5 genome through PacI digest. After digestion, the genome was transfected into HEK293 cells, and we waited to observe cytopathic effects (CPE). Roughly 7 days post transfection, we observed clear cell rounding and death, indicating the potential presence of virus. Viral infection was expanded to a cell factory to perform CsCl purification. To avoid potential reversion to wild type adenovirus through recombination, E1 complementing N52 cells that have minimal areas of homology with the HAd5 genome were utilized during viral expansion [77]. After purification, to confirm whether our transgene was still present within the virus, we performed a viral DNA extraction and PCR. These primers utilized were not specific to CanH3 Mosaic, but to the CMV promoter and SV40 polyadenylation site flanking the gene. PCR produced a

2000 kbps product, roughly the size of our transgene expression cassette, confirming the presence of the CanH3 mosaic within viral DNA (Figure 3.3b).

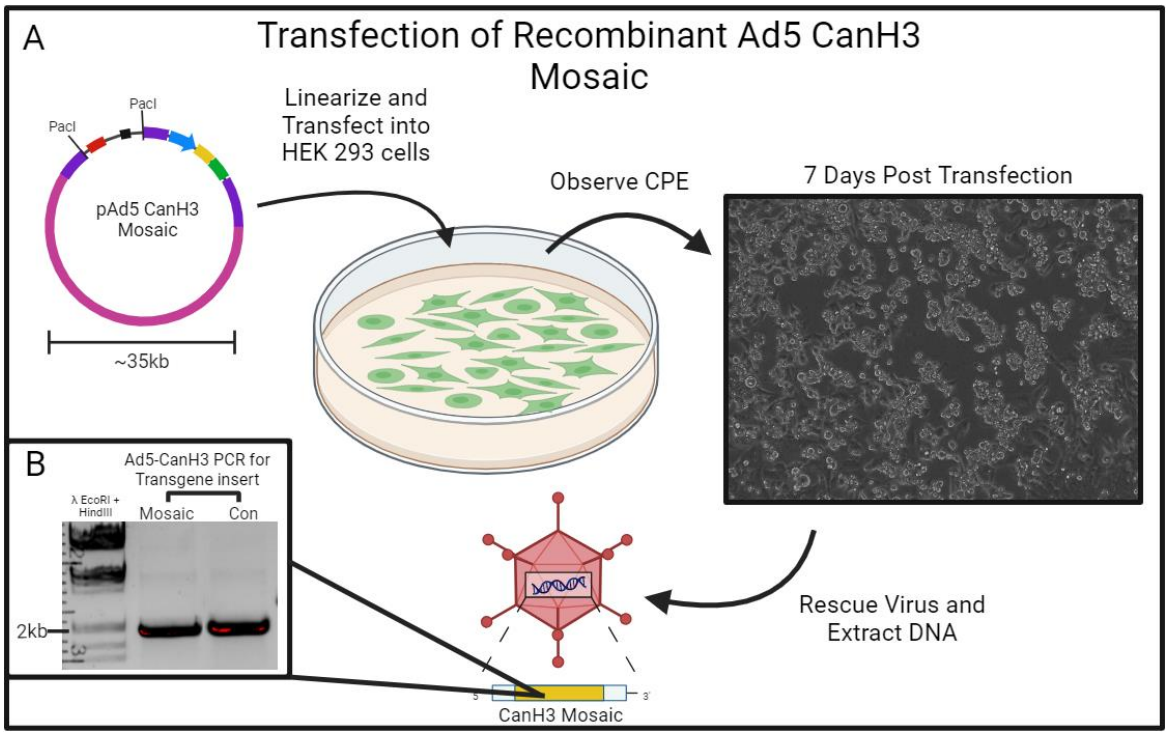

Figure 3.3: HAd5-CanH3 Transfection and Confirmation: *(A) pAd5-CanH3 is first linearized through PacI digest, before being transfected into E1 complementing HEK 293 cell. A week after transfection, CPE was observed in the cells. Following observation of CPE, the virus was grown up and purified. (B) After purification, viral DNA was extracted and PCR for the entire transgene, including the CMV promoter and SV40 PA site, was performed. PCR was positive for a 2 kbp band, indicating presence of our transgene.*

DISCUSSION

Adenovirus vectors are an inviting avenue for vaccine development. The decades of research behind understanding the transcriptional cascade of the genome, have allowed

for precise modification of the virus and transgene insertion [66, 68]. Therefore, these vectors can easily be rendered replication-defection through the deletion of essential genes such as E1, making these vectors safe and low risk options for vaccines [65]. The broad tropism of adenoviruses only aids in the appeal as it increases the potential routes of delivery that can produce transgene expression, for example, oral, intramuscular, or intranasal [65, 68]. This is only reinforced by scalability and ease of access since these vectors are grown in cell lines. As HAd5 is one of the most commonly used Ad vectors due to its very high immunogenicity, methods for vector development are also well described and commercially available [66]. HAd5 vectors also have the potential to induce high transgene expression in dogs [73-75]. Therefore, we chose to develop our CIV vaccine using an HAd5 vector.

In this chapter we demonstrated in detail the pAdEasy system which we used to construct replication defective HAd5 with our CanH3 mosaic inserted into the E1 gene. This system, first developed by He, et al, uses a series of plasmids, pShuttle-CMV and pAdEasy to move a desired transgene into the E1 locus of HAd5 [67]. We demonstrated that we inserted our transgene into pShuttle-CMV with T4 ligation through restriction digest. We further “shuttled” our transgene into the HAd5 E1 through homologous recombination in BJ5183 cells. This renders our recombinant replication defective. Restriction digest and whole plasmid sequencing confirmed we had produced a successful recombinant. Additionally, to demonstrate this recombinant could produce virus, we linearized and transfected the HAd5 Mosaic CanH3 genome into E1 complementing HEK293 cells and were able to detect CPE. After viral purification, the presence of our transgene was confirmed through PCR. However, screening for

replication competent adenovirus within our viral sample must be performed, as it is possible for recombinant HAd5 to revert back to wild type when using HEK293 cells [68]. Despite confirming the presence of the gene, expression has not yet been clearly demonstrated. We did perform a western blot and that appeared to be positive for CanH3 Mosaic expression, but the GAPDH positive control was negative. Further analysis through western blot testing should be done to fully confirm expression of the CanH3 Mosaic before testing in animal models.

Our goal is to develop a CIV vaccine that can induce a broadly protective immune response. In our previous chapter we discussed how our Mosaic CanH3 was constructed to maximize the potential T cell epitopes within a single immunogen. This theoretically can broaden and enhance the immune response generated against the vaccine. With HAd5 inherently being a respiratory pathogen, matching influenza, intranasal delivery could be a very promising avenue for providing protection. The viral nature of the vector itself, paired with the high immunogenicity of the HAd5 vector could help induce a very strong antiviral response to our vaccine and immunogen [78]. However, the HAd5 vectored system is not without its drawbacks. Vaccination often not only creates immune reactions against the target transgene, but the vector itself [68]. This could potentially limit the frequency in which specific adenovirus vectors are used to vaccinate [72]. If adenovirus vectored vaccines become commercially available, a multitude of adenoviral vectors should be utilized to circumvent vector immunity. Another consideration is preexisting immunity, which could limit the effectiveness of these vaccines in populations with high preexisting immunity [68]. The vector we opted to utilize is a human adenovirus and thus theorized to have low seroprevalence in dogs. HAd5 has a

reported 80% seropositivity in some human populations [68]. Since dogs commonly serve as companion animals, there is concern there could be some cross-over in this seropositivity. Few studies have assessed the prevalence of HAd5 neutralizing antibodies in dogs, therefore we propose that further studies be done to analyze the impacts this may have. Human adenoviruses also demonstrate transformative properties in cell culture and unnatural hosts [79]. As adenoviral induced tumorigenesis has mainly been observed in rodents and the oncogenic E1 gene has been removed from our vector, we theorize this issue to be minimal [79]. Yet, this remains an important avenue to be investigated in order to ensure the safety of HAd5 vectors in dogs. Another risk that comes with using a viral vector is the potential for cross species transmission. Our constructed HAd5 vector is rendered replication defective through E1 gene deletion, but replication competent adenovirus is always a potential contaminant when developing these vectors. Therefore, extensive quality controls measures must be adopted to limit contamination.

Overall, we outline the steps we took to insert our CanH3 mosaic immunogen into an HAd5 vector, utilizing the pAdEasy vector system. Growth of the recombinant virus and the presence of our transgene were also confirmed. When we are able to detect expression of our transgene in vitro, we plan to move into mouse models to begin the preliminary steps in testing the efficacy of our vaccine in vivo.

METHODS

Insertion of CanH3 Mosaic into pShuttle-CMV

To remove our mosaic gene from pFastBacI, we NotI and HindIII digested 5 μg of the plasmid at 37 °C for 1 hour. Following digestion, the products were run on a 0.8%

agarose gel. The 1.7 kbp band corresponding to the CanH3 Mosaic was gel extracted using the QIAquick Gel Extraction Kit (QIAGEN). pShuttle-CMV was also digested with NotI and HindIII 37 °C for 1 hour, products were cleaned up with Agilent Technologies StrataPrep PCR purification kit. 50 ng of digested pShuttle-CMV and 37.5 ng of CanH3 mosaic were used for T4 ligation, following manufacturers protocol (New England Biolabs) and left to react overnight at 4 °C. 1 μL of the ligation reaction was electroporated into 45 μL of XL-1 cells. Cells were then rescued in 550 μL of S.O.C. media for 1 hour before 20 μL and 200 μL were plated onto LB+Kan plates. Plates were left to incubate overnight 37 °C. Five single colonies were selected from the plates and grown separately in 3 mL of LB + Kan media (50ng Kan per mL of media) at 37 °C in shaker overnight. Plasmid DNA was isolated from samples using the QIAprep Spin Miniprep Kit, following manufacturers protocol. Confirmation for successful ligation was tested through NotI and HindIII digesting plasmid DNA and assaying for the 1.7 kbp transgene insert. Digests were run on 0.8% agarose gel for 30 minutes at 130V and imaged with ethidium bromide and UV fluorescence.

Insertion of CanH3 Mosaic into pAdEasy

4 μg of pShuttle-CMV CanH3 mosaic was digested with 4 μL of PmeI (10,000 units/ml) at 37 °C for 1 hour to linearize. Sample was dephosphorylated using 4 μL of Antarctic phosphatase following manufacturers protocol (NEB). PmeI digested pShuttle-CMV was electroporated at 2500V into 45 μL of BJ5183 cells along with pAdEasy in a 1:2 nanogram ratio. Cells were rescued in 550 μL of S.O.C. media at 37 °C in the shaker for 1 hours. 20 μL and 200 μL were then plated on LB + Kan plates and left to incubate 37

°C overnight. Eight single colonies were then selected and grown in 3 mL of LB + Kan media. Plasmid DNA was extracted using QIAprep Spin Miniprep Kit, following manufacturer protocol. Plasmid DNA was then digested with PacI before being run on a 0.8% agarose gel at 130V for 30 minutes. Plasmid DNA from lanes that appeared empty were selected for further analysis. Selected plasmid DNA samples were electroporated into 45 μL of XL-1 cells at 2500V volts. Cells were rescued in 550 μL of S.O.C. media before 20 and 200 μL were plated on LB + Kan plates. Plates were incubated at 37 °C overnight. Two single colonies were selected and used to inoculate 150 μL of LB + Kan media, then incubated overnight in shaker at 37 °C. Plasmid DNA was then isolated using HiSpeed Plasmid Midi Kit (QIAGEN). Samples were digested with PacI and run on a 0.8% agarose gel. Samples that had two fragments, one around 35 kbps and the other around 3.5 kbps were selected for further analysis.

Whole Plasmid Sequencing

30 μL of potential pAd5 CanH3 Mosaic samples were placed into 1.5 mL microcentrifuge tubes before being mailed to Eurofins Genomics for Whole Plasmid Sequencing. Upon receiving the results, sequences were analyzed using MacVector. The HA sequence from the sequenced plasmid was then aligned using ClustalW to our CanH3 Mosaic sequence.

Transfection of pAd5 CanH3 mosaic into HEK 293 cells

2 μg of pAd5 CanH3 Mosaic was PacI digested at 37 °C overnight. Following digestion, products were cleaned up using Agilent Technologies StrataPrep PCR purification kit. Sample was then mixed with DMEM (-/-) up to 200 μL and 40 μL of Polyfect. The

sample was vortexed and allowed to incubate at room temperature for 10 minutes. Media was removed from 50-70 confluent HEK293 cells in a 6 well plate and replaced with 1.5 mL of DMEM with 10% FBS and 1% P/S. After 10-minute incubation, 660μL of DMEM (-/-)) was added. 500 μL of the mixture was added to 2 wells and left to incubate at 37 °C. Media was replaced every 4 days until CPE was observed. Cells were washed off plate and spun down in centrifuge at max for 1 minute. The sample was freeze thawed 3 times and then centrifuged at max for 1 minute. Supernatant was used to infect N52 cells. Infection was expanded into a Cell Factory, followed by CsCl purification to isolate the recombinant HAd5 CanH3 Mosaic.

PCR to confirm presence of Transgene within recombinant HAd5

After CsCl purification, viral DNA was isolated using PureLink Viral RNA/DNA Mini Kit (Invitrogen). Following extraction, the primers 5' GGTCTATATAAGCAGAGCTGG 3' and 5' GTGGTATGGCTGATTATGATCAG 3' were used for PCR amplify up the transgene, including the CMV and pA. NEB Q5 High Fidelity DNA Polymerase was used according to manufacturer's protocol. Resulting PCR products were run on a 0.8% agarose gel at 130V for 30 minutes. Gel results were imaged with ethidium bromide and UV fluorescence.

CHAPTER 4: DEVELOPMENT OF A CAV-2 VECTOR SYSTEM

INTRODUCTION

In the early 20th century, infectious canine hepatitis was first observed in dogs [80]. This disease, often more fatal in younger dogs, is often associated with fever, abdominal pain, diarrhea, vomiting, and in some rare cases, respiratory and neurological distress [80]. During recovery, iridocyclitis is often an indicator of recent infection [80, 81]. It was not until the mid-20th century that the causative agent, Canine Adenovirus Type 1 (CAV-1), was identified [80]. The host range of this virus is surprisingly broad, including dogs, wolves, foxes, otters, brown bears, and coyotes [81]. CAV-1's incubation period is often between 4-9 days depending on whether it was contracted through direct contact, or by ingesting infected material [80, 81]. The mortality rate ranges from 10-30% and it is often elevated further during coinfection with other pathogens [80]. Interestingly, despite recovering clinically from the infection, dogs can still secrete CAV-1 in urine for up to 9 months post infection [80].

In 1961, a new type of canine adenovirus would be isolated, Canine Adenovirus Type 2 [80]. Immune responses against type 1 and 2 are cross protective, leading to CAV-2 initially being considered an attenuated form of CAV-1 [81]. However, some differences were identified over time. These viruses only shared 75% nucleotide identity and had distinct pathologies, leading to the classification of CAV-2 as its own separate virus [80]. CAV-2 is now clinically associated with a complex of viruses known to cause kennel cough or tracheobronchitis, as it replicates more efficiently in the respiratory tract when compared to CAV-1, which instead prefers renal and vascular endothelial cells [80]. Since CAV-2 is often associated with less severe disease than CAV-1, recombinant

Canine Adenovirus Type 2 (CAV-2) vectored vaccines have been utilized as an effective and safe delivery system for recombinant proteins in animals [82-87].

Similar to other adenoviruses, CAV-2 has a broad cellular tropism, allowing the potential delivery of CAV-2 vectors through multiple routes [83]. The oral route has been particularly inviting, as baits containing the vaccine can be developed to easily vaccinate stray dog populations [83]. Recombinant CAV-2 expressing a rabies G protein disguised as a bait induced protective antibody titers that lasted 2 years in 90% of dogs vaccinated, showing the potential of this vector to produce long lasting protective immunity in dogs [83]. Replication competent E3 deleted (ΔE3) variations of the CAV-2 vector have been utilized to induce immune responses in raccoons, skunks, dogs, sheep, and mice to provide protection against rabies, foot and mouth disease, canine distemper virus, and canine influenza virus [82-87]. While less common, Replication defective E1 deleted (ΔE1) CAV-2 vectors have been used in sheep and guinea pigs to induce humoral and cell mediated protection against rabies and foot and mouth disease [82, 88]. While these vaccines do not always illicit as robust of an immune response as live attenuated vaccines, they provide a protective, safe, and effective way to administer antigens as they do not infect humans and CAV-2 replicates efficiently in dogs [82, 83, 88].

As an E3 deleted, CAV-2 vectored CIV vaccine has already been developed, we plan to improve on this by delivering a computationally derived Mosaic CanH3 in an E1 deleted CAV-2 vector. A CAV-2 vectored CIV vaccine will have the additional advantage of potentially immunizing not only against CIV, but against both subtypes of canine adenovirus. While systems for creating recombinant CAV-2 have been developed, they are not commercially available [89]. Therefore, in this chapter, we outline the methods

which we used to develop our CAV-2 vector system. We employed an approach, similar to the pAdEasy vector system, to insert our transgene expression cassette into CAV-2 through homologous recombination of a shuttle and genomic CAV-2 plasmid [67]. Generation of our shuttle and recombinant plasmids were developed by utilizing Gibson assembly, overlapping PCR, and minimal restriction digest cloning. We confirmed the construction of plasmids that can later be used to create recombinant CAV-2 through restriction digest and whole plasmid sequencing.

RESULTS

To construct our recombinant CAV-2, we developed a system similar to pAdeasy (Figure 4.1). This system involves two plasmids, a CAV-2 shuttle plasmid and a genomic CAV-2 plasmid. After inserting a transgene into the CAV-2 shuttle plasmid, it can be moved into the genomic plasmid using homologous recombination. The shuttle plasmid contains sites of homology with the CAV-2 genome that flank the left and right of the E1 gene. Therefore, during homologous recombination, the transgene will be inserted into the CAV-2 E1. This system will then theoretically create a replication defective CAV-2 expressing our CanH3 transgene.

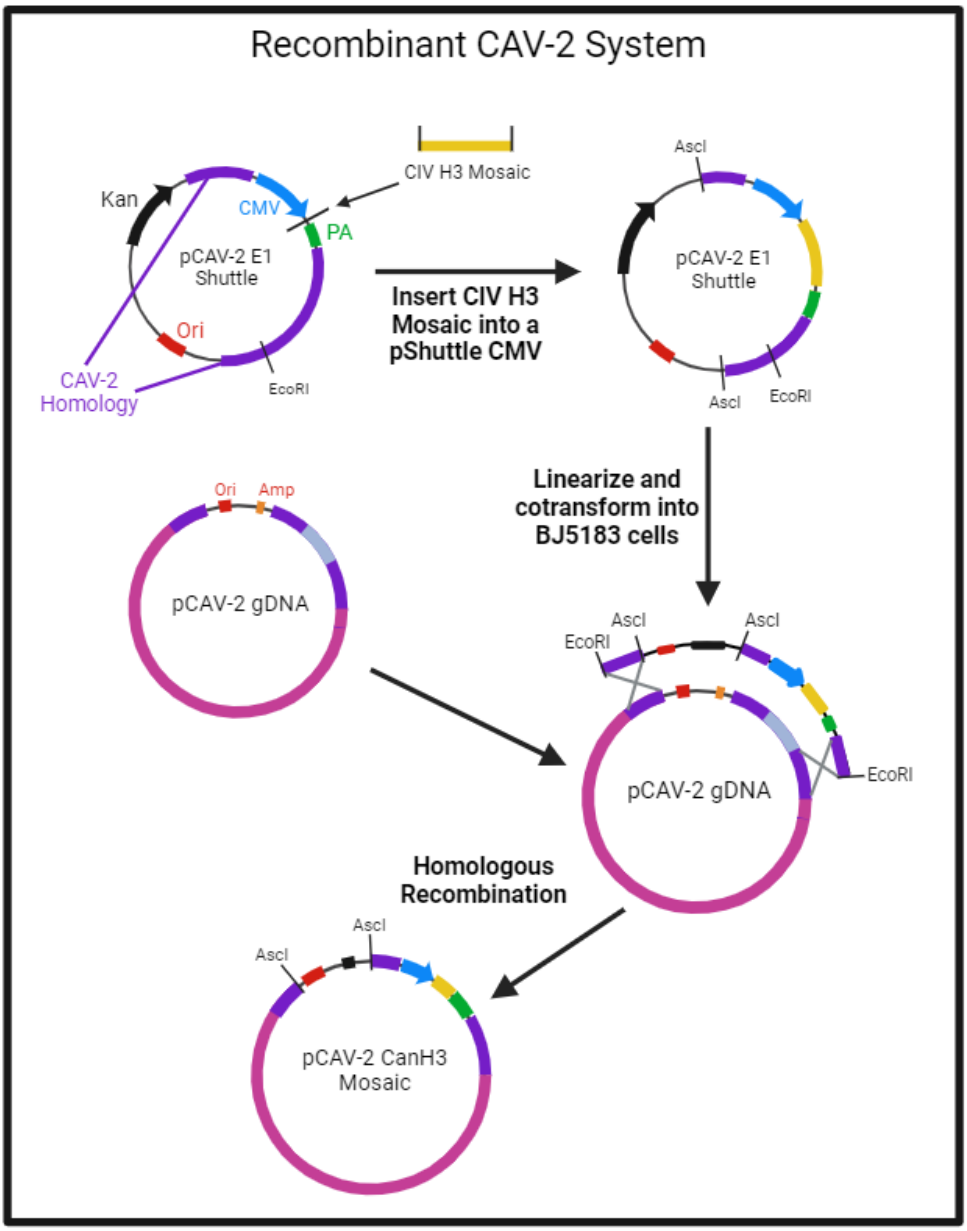

Figure 4.1: Recombinant CAV-2 System: *This recombinant CAV-2 system is modeled after the pAdEasy system. The first step is to insert the desired transgene into the CAV-2 shuttle plasmid. This plasmid contains areas of homology with the genomic CAV-2 plasmid. After insertion of the transgene, the shuttle is then linearized by EcoRI digestion and co-transformed into BJ5183 cells for homologous recombination. Recombination*

inserts the transgene into the E1 locus, and the replication defective vector can be linearized with AscI for further use.

Isolation of Canine Adenovirus Type 2

Before construction of a CAV-2 vector system could begin, we had to grow up and isolate the virus, to have a reliable source of CAV-2 DNA. We obtained an infected lung sample supplied by the Colorado State Veterinary Diagnostic Center. This sample, from 2018, originated from a 3-month-old border collie mix from Arizona that had tested positive for CAV-2, but negative for other common respiratory ailments such as canine distemper virus and canine influenza virus. After receiving the sample, a small piece was homogenized in DPBS and filtered through a 0.2 um filter to remove bacterial contaminants, before inoculating Madin-Darby canine kidney cells (MDCK). The inoculated cells developed signs of CPE over the next 4 days (Figure 4.2a). PCR specific to the CAV-2 hexon was used to confirm the presence of the virus (Figure 4.2b). The PCR shows a clear positive for CAV-2 hexon DNA in the infected MDCK sample, and negative in both a genomic HAd5 and MDCK control (Figure 4.2b). PCR confirmed the presence of CAV-2 within our sample, and therefore we expanded viral replication into a cell factory and purified virus using CsCl centrifugation (Figure 4.2c). A large viral particle band formed during purification, and we ended up with a concentration of roughly 1.68 e^{13} vp/mL.

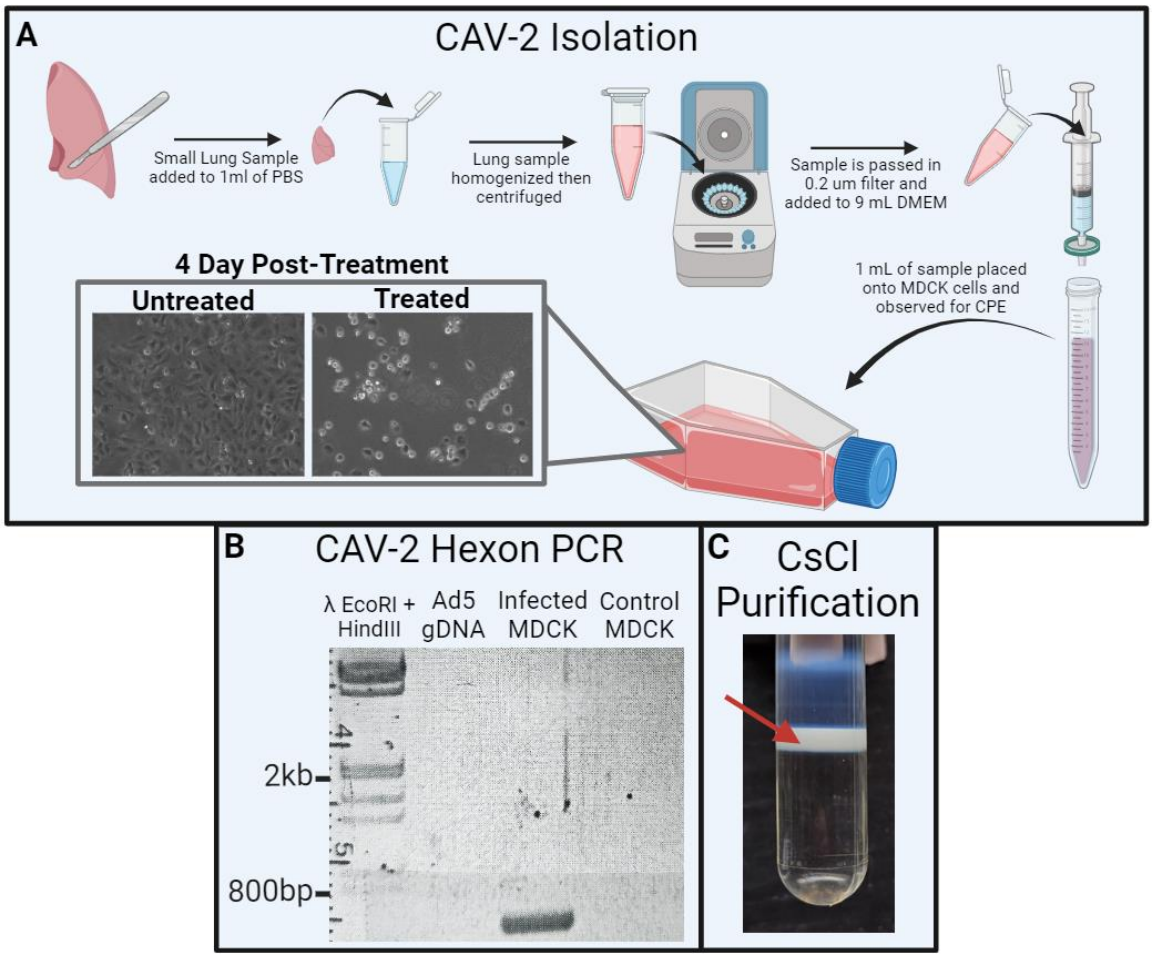

Figure 4.2: Isolation of Canine Adenovirus Type 2: *(a) Outline for the steps taken to isolate CAV-2. We first homogenized a small lung sample in PBS, before centrifuging. The supernatant was then filtered through a 0.2 um filter to remove any bacterial contaminants. The sample was mixed with media and used to inoculate MDCK cells. Four days post treatment, CPE was observed. (b) PCR specific to the CAV-2 hexon was used to confirm the presence of CAV-2. The infected MDCK cells showed a clear positive for PCR, while the HAd5 gDNA and untreated MDCK control were both negative. (c) The viral particle band obtained through CsCl centrifugation. The red arrow marks the location of the band.*

Development of the CAV-2 genomic plasmid

The genomic CAV-2 plasmid (pCAV-2 gDNA) was constructed utilizing Gibson Assembly. Gibson assembly, originally developed by Daniel Gibson in 2009, is a cloning method that is used to ligate separate DNA molecules together (Figure 4.3) [90]. As long as the DNA molecules contain a minimum of a 20-base pair overlap, they can be joined in a single isothermal reaction [91]. This required overlap between DNA molecules is often added through PCR. The first step of Gibson Assembly involves a T5 exonuclease [92]. This exonuclease cleaves back the 5' ends of the DNA double strands to uncover the overlaps added by PCR [92]. The two separate strands then anneal via these complementary overlaps. Filling in the gaps formed as a result of excessive endonuclease activity is initiated by a DNA polymerase and finished off by a DNA ligase [90].

pCAV-2 gDNA was assembled with Gibson assembly, through the ligation of a PCR product, containing an ampicillin resistance gene (Amp) and an origin of replication (Ori), with genomic CAV-2 DNA (Figure 4.4a). The PCR was used to amplify the Ori and Amp from pAdEasy, add overlaps homologous to the ends of CAV-2, and AscI restriction sites (Figure 4.4b). CAV-2 genomic DNA was isolated from previously purified CAV-2. The Amp + Ori PCR product along with genomic CAV-2 were mixed in a 1:2 nanogram ratio, before performing Gibson Assembly according to the manufacturer's protocol. Following ligation and electroporation into electrocompetent XL-1 cells, ten bacterial clones were obtained. Two of the clones selected were positive for PCR specific to the CAV-2 hexon (Figure 4.4c). Following PCR, plasmids were isolated from the bacterial samples and AscI digested for further confirmation of plasmid construction (Figure 4.4c). Restriction digestion produced two expected bands sized

approximately 3500 bp, which corresponds to the Amp + Ori fragment, and 31500 bp, which corresponds with genomic CAV-2 DNA.

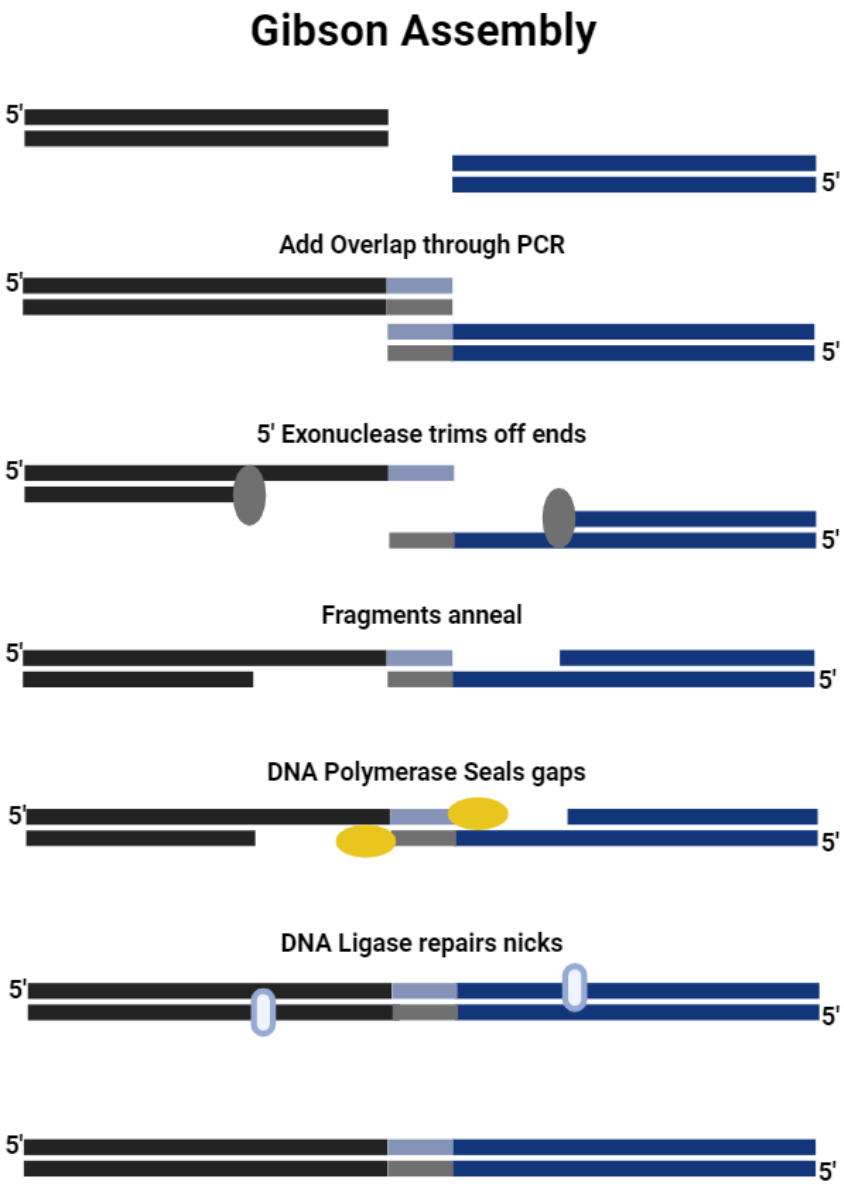

Figure 4.3: Gibson Assembly Reaction: A figure partially adapted from Snapgene Gibson Assembly guide (https://www.snapgene.com/guides/gibson-assembly), Gibson assembly can ligate two DNA molecules with a minimum of a 20 bp overlap. PCR can easily be used to add overlaps. Ligation is achieved through three enzymes. First an Exonuclease

trims off the 5' ends, followed by annealing of the fragments. DNA polymerase is used to seal gaps and a DNA ligase will repair the leftover nicks [90, 92].

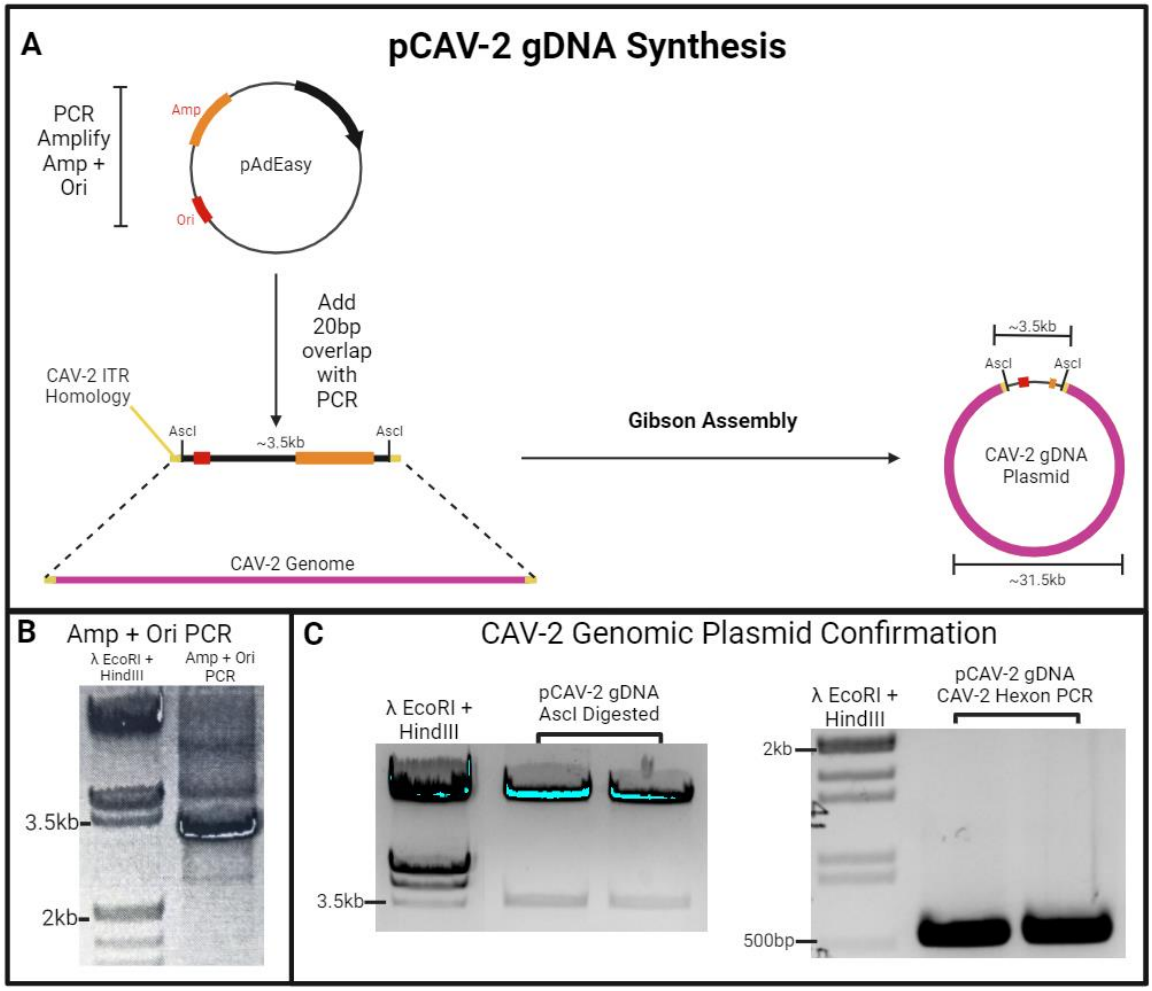

Figure 4.4: Construction of pCAV-2 gDNA: (a) The genomic CAV-2 plasmid was constructed using Gibson assembly. First an ampicillin resistance gene and origin of replication were amplified from pAdEasy. This PCR was used to add overlaps with the ends of the CAV-2 genome, along with AscI restriction sites. After PCR, the product was mixed with full length CAV-2 genome for Gibson Assembly to create pCAV-2 gDNA. (b) The Amp + Ori PCR product. It is approximately 3.5 kbps in size. (c) AscI restriction digest, along with PCR specific to the CAV-2 hexon were used to confirm pCAV-2 gDNA

construction. On the left, AscI digestion produced two bands for both potential plasmids, a 3.5 kbp fragment, which corresponds with the Amp + Ori, and a 35-kbp product that corresponds to the full-length CAV-2 genome. On the right, the two potential plasmids were both positive for the CAV-2 hexon.

To further confirm construction of pCAV-2 gDNA, the assembled plasmid was sent in for whole plasmid sequencing (Figure 4.5). Results from sequencing show a full-length CAV-2 genome, along with an Amp + Ori flanked by two AscI sites. The sequenced plasmid is roughly the same size as the expected plasmid, with only a three base pair increase (Figure 4.5a). Full genome alignment between the sequenced CAV-2 genome and a previously sequenced Toronto/1961 CAV-2 isolate showed these genomes were 99.9% identical, with a 20-nucleotide divergence. This comparison also revealed that the discrepancy in the plasmid size is a result of a three base pair insertion within the fiber coding region. To minimize the chance the nucleotide changes were due to sequencing error, we sequenced our genomic plasmid two additional times. The base pair insertion in the fiber only appeared within the original sequencing results, potentially showing it was a result of a sequencing error. However, ten differences were present in all three sequencing results, with six potentially resulting in amino acid changes (Figure 4.5b). Exact nucleotide and protein location, along with potential nucleotide and amino acid change are detailed in Table 4.1.

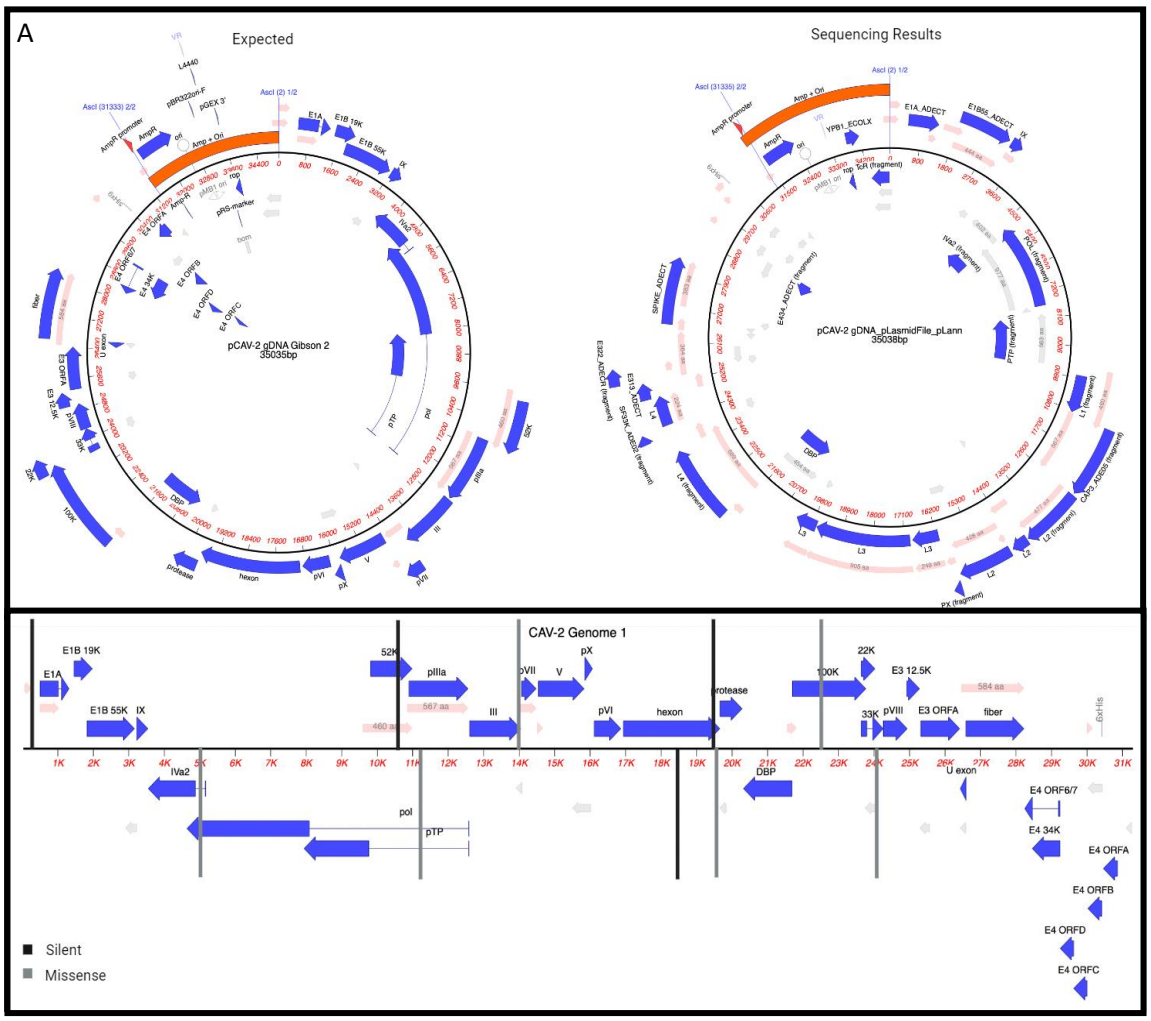

Figure 4.5: Sequencing of pCAV-2 gDNA: (a) On the left is a pCAV-2 gDNA constructed within MacVector using the Gibson Assembly function. On the right is the result of whole plasmid sequencing for pCAV-2 gDNA. There is a three base pair difference in size between the expected and sequenced plasmid. (b) The entire CAV-2 genome annotated with differences present in all three sequencing results of the captured CAV-2 genome within pCAV-2 gDNA. Six of the ten mutations potentially result in an amino acid change.

Location	**Nucleic Acid Position**	**Change**	**Potential Amino Acid Change**
Psi packaging signal **[93]**	299	C to G	N/A
Polymerase **[94]**	5057	C to T	Ser to Leu
52k encapsidation protein **[94]**	10515	C to T	Silent
pIIIa minor capsid protein **[95]**	11195	TGTG to GTGT	Cys to Val Ala to Ser
III Penton Base **[95]**	14024	C to T	Ala to Val
Hexon major capsid protein **[95]**	18414	G to A	Silent
	19605	T to G	Silent
	19616	G to T	Gly to Val
100K hexon assembly protein **[95]**	22568	C to T	Arg to Cys
33k packaging protein **[95]**	24064	C to A	Leu to Ile

Table 4.1: Sequencing discrepancies between Arizona 2018 CAV-2 isolated and Toronto 1961 isolate: *Discrepancies present in all three sequencing results of the pCAV-2 gDNA are listed within this table, along with exact location, nucleotide change, and potential amino acid change.*

Development of ΔE1 CAV-2 Shuttle Plasmid

To construct our ΔE1 CAV-2 Shuttle Plasmid, we employed a combination of Gibson assembly and overlapping PCR. Since our plasmid is modeled after pShuttle-CMV from the pAdEasy system, our shuttle plasmid is constructed through the assembly of five components: 500 bps left of CAV-2 E1 (Left E1), a major cloning site (MCS) flanked by a CMV promoter and polyadenylation signal (CMV MCS), 500 bps right of CAV-2 E1 (Right E1), the 500 bps at the end of the CAV-2 genome (End CAV-2), and a fragment containing a kanamycin resistance gene (Kan) plus an origin of replication (Ori) (Kan + ori). All fragments were first PCR amplified to add overlaps to the fragments that would be adjacent in the final construct. The Left E1, Right E1, and End CAV-2 were amplified from CAV-2 genomic DNA, while the CMV MCS and the Kan + Ori fragment was amplified from pShuttle-CMV. A pair of AscI restriction sites were also added to the ends of the Kan + Ori fragment during PCR. After PCR, the Left E1, CMV MCS, Right E1, and End of CAV-2 were joined together using overlapping PCR (Figure 4.6). Following overlapping PCR, the product was ligated to the Kan + Ori fragment through Gibson assembly. Following ligation and electroporation into electrocompetent XL-1 cells, two bacterial colonies were obtained. Plasmid DNA was extracted from bacterial samples and AscI digested to confirm construction of the plasmid (Figure 4.7a). Restriction digestion produced two bands slightly smaller than the expected bands of 2.9 kbp, which corresponds to the Kan + Ori fragment, and 2.3 kbp, which corresponds with the overlapping PCR product (Figure 4.7a). The bands were close to their expected sizes, so we proceeded with sequencing.

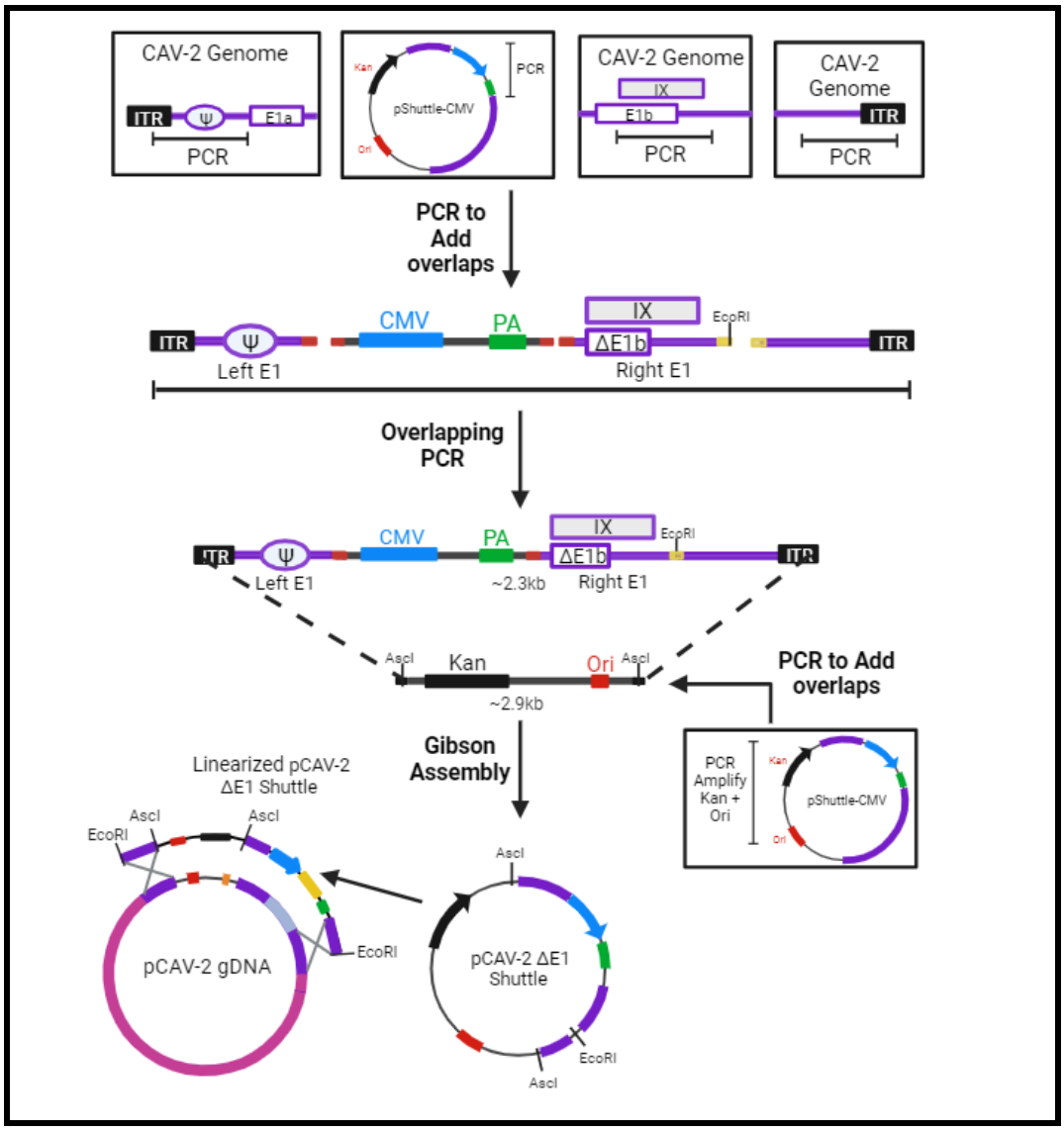

Figure 4.6: ΔE1 CAV-2 Shuttle Plasmid Development: *Schematic that shows the steps used to construct the ΔE1 CAV-2 Shuttle Plasmid. The first step is to PCR amplify all fragments to add 20 bp overlaps. Following amplification, fragments were joined through overlapping PCR. PCR was then used to amplify the Kan + Ori from pShuttle-CMV and add ascI sites along with a 20 bp overlap with the overlapping PCR product. The overlapping PCR product along with the Kan + Ori fragment were then joined through overlapping PCR. This plasmid can then be linearized with EcoRI for future co-transformation into BJ5183 cells and recombination with pCAV-2 gDNA. It is important*

to note that there was an EcoRI site at the end of the Right E1 fragment, therefore it did not have to be added during PCR.

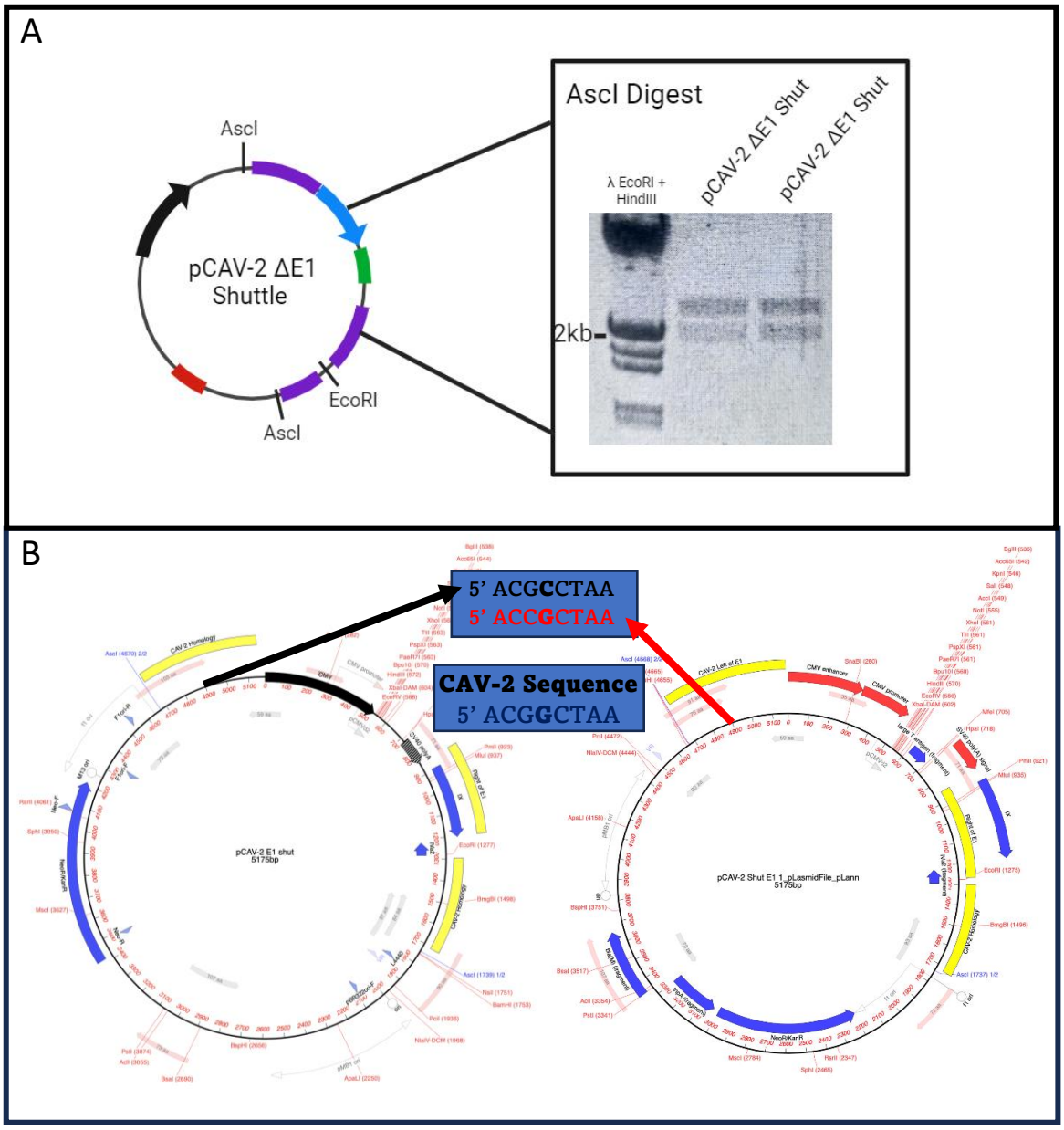

Figure 4.7: Confirmation of ΔE1 CAV-2 Shuttle Plasmid construction: *(a) After Gibson Assembly, to confirm construction of the plasmid, it was AscI digested. AscI digestion produced two bands slightly smaller than expected. (b) On the left is the expected ΔE1 CAV-2 Shuttle Plasmid, on the right is the whole plasmid sequencing*

results for the potential plasmid. Sequencing shows that the plasmids are nearly identical except for a single nucleic acid change within the left E1 fragment, and an inversion of the kan + ori fragment. This single base pair difference was also present in our CAV-2 whole genome sequencing results, indicating the difference was due to using our 2018 isolate as a template for PCR.

To further confirm construction of the ΔE1 CAV-2 Shuttle Plasmid, we once again utilized whole plasmid sequencing (Figure 4.7b). Sequencing revealed a plasmid with an identical size to the expected plasmid of 5175 bp. There were two differences noted, however. The first change is a single nucleotide difference within the left E1 fragment, from C to G (Figure 4.7b). As this nucleotide change was also present within our genomic CAV-2 sequencing results, the difference is most likely a result of using it as a template for PCR. The other difference was an inversion of the Kan + Ori fragment. As the 20-base pair overlaps between the Kan + Ori fragment and the overlapping PCR product are within the CAV-2 ITRs (Figure 4.6), the fragment could potentially insert either way. Adenovirus ITRs, or inverted terminal repetitions, are identical and located on both ends the genome [96]. Therefore, the ends of the Kan + Ori fragment are homologous to both ends of the CAV-2 genome, allowing the Kan + Ori fragment to potentially ligate either way during Gibson assembly. The results from whole plasmid sequencing showed we had constructed the target CAV-2 shuttle plasmid.

DISCUSSION

In this chapter, we outlined the methods in which we used to construct our CAV-2 vector system. This system is modeled after the pAdEasy vector system for HAd5 [93]. We first constructed a genomic CAV-2 plasmid (pCAV-2 gDNA) by ligating a PCR product containing an ampicillin resistance gene and origin of replication with genomic CAV-2 DNA through Gibson Assembly. Following this, a ΔE1 CAV-2 Shuttle Plasmid was constructed utilizing both overlapping PCR and Gibson assembly. Results from whole plasmid sequencing along with restriction enzyme digestion supported the successful construction of these plasmids. The next step would be to insert the desired transgene into the MCS of the ΔE1 CAV-2 Shuttle Plasmid. Following insertion, due to the areas of homology left and right of the E1, homologous recombination can theoretically be used to insert a transgene into the E1 coding regions of the pCAV-2 gDNA plasmid (Figure 4.1). All of the plasmids required for a recombinant ΔE1 CAV-2 system have been constructed.

Once construction of a recombinant ΔE1 CAV-2 is confirmed, further progress will be hindered until a CAV-2 E1 complementing cell line is developed. As E1 is a necessary transcription factor, deletion inhibits the growth of the virus [77]. The E1 gene appears to vary enough between adenoviral species that only select E1 genes can be used to propagate E1 deleted adenoviruses [77]. Therefore, we are limited in our use of other Ad E1 complementing cell lines and must develop one specific to CAV-2. Other labs that have generated recombinant CAV-2 have also relied on specific CAV-2 E1 complementing cells for viral amplification [89]. Developing a CAV-2 E1 complementing cell line remains a priority for future studies.

When compared to previously available methods, whole plasmid sequencing through Eurofins genomics provides a rapid and relatively low-cost way to evaluate a plasmid. It costs $15-30 dollars per sample, depending on size, and results are available within a couple days. It is particularly useful in verifying the construction of a specific plasmid during cloning, as we used it to verify both the pCAV-2 gDNA plasmid and the ΔE1 CAV-2 shuttle plasmid. While divergence from what is expected in our shuttle plasmid can be readily explained, differences in the pCAV-2 gDNA cannot. To minimize the chance that differences were due to sequencing error, pCAV-2 gDNA was sequenced three times. Ten differences from the reference Toronto 1961 strain were present in all three results, with six potentially resulting in amino acid changes. Our isolate was originally isolated in 2018, 57 years after the reference strain. Therefore, these differences can be a result of mutation over time. This opens many potential avenues to explore how these mutations affect the lifecycle of this virus. However, it cannot be ruled out that these changes could be due to sequencing error, growth in cell culture, or mutation during bacterial cloning. The most relevant question is whether these mutations will affect the growth of our future recombinant CAV-2 developed from this plasmid. We plan to confirm if our cloned CAV-2 genome is infectious through linearization and transfection into MDCK cells. We expect to see clear signs of infection, such as cell rounding and detachment, within 1 to 2 weeks of transfecting the genomic CAV-2 DNA.

In regard to delivering our CanH3 mosaic using this vector, preexisting immunity could potentially hinder the impacts of a CAV-2 vectored vaccine. While seroprevalence of CAV-2 tends to vary in dog populations, it appears to be the highest in dog populations with high levels of interaction [97, 98]. As these dog populations are the most at risk of

contracting CIV, this is mostly likely the biggest limitation of a CAV-2 vectored CIV vaccine [36, 81]. However, changing the route of delivery is a promising way to circumvent this. A study performed by Fischer et al showed that while intranasal immunization with a recombinant CAV-2 was hindered by preexisting immunity, a subcutaneous vaccination was not [86]. Other alternatives such as coating the virus with polymers, or targeting the vaccine toward young, immunologically naïve dogs could be other ways to minimize the issue [68, 86]. We further plan to use the ability of this vector to induce immunity against CAV-2 as a strength, making our vaccine induce protection against both CIV and CAV-2 [83].

Overall, we demonstrated the steps used to develop our recombinant CAV-2 system. We generated both a genomic CAV-2 plasmid and a ΔE1 CAV-2 shuttle plasmid. Whole Plasmid sequencing was used to verify construction and it showed Gibson assembly and overlapping PCR were effective methods to develop these plasmids. In the future, we plan to test the ability of this system to develop a recombinant CAV-2 expressing our CanH3 Mosaic. As CAV-2 and CIV affect very similar populations of dogs, we plan to test the ability of these vaccines to protect these dogs from both [36, 81].

METHODS

Cells, Enzymes, Plasmid and Bacteria

MDCK cells utilized in this study were previously preserved in our lab and grown in DMEM 5% FBS and 1% P/S. XL-1 competent cells were made by growing E. coli to A600 before washing twice in MilliQ water and freezing at -80°C. Restriction enzymes used were purchased from New England Biolabs (NEB). All PCR was performed using

NEB Q5® High-Fidelity 2X Master Mix according to NEB protocol. The NEBuilder® HiFi DNA Assembly Master Mix used for Gibson assembly was purchased from New England Biolabs. The pShuttle-CMV and pAdeasy plasmids used for PCR were available from the Agilent Technologies AdEasy Adenoviral Vector System. All theoretical plasmids and overlapping primers were developed utilizing the Gibson Assembly program within MacVector and primers were ordered through Eurofins Genomics

Canine Adenovirus Type 2 Genomic Isolation

The Canine Adenovirus Type 2 sample used for our studies was isolated from infected dog lung and spleen samples from a 3-month-old border collie mix from Arizona. These tissue samples were PCR positive for CAV-2 and supplied by the Colorado State Veterinary Diagnostic center. After the samples were received, a scalpel was used to detach a small sized sample. This sample was placed in a 1.5mL microcentrifuge tube with 1 mL of DPBS. The PBS and Sample mixture was homogenized and followed with centrifugation at maximum speed for 1 minute. The proceeding supernatant was filtered through a 0.2 um filter. The filtered supernatant was added to 9 mL of DMEM 5% FBS and 1% P/S. 1 mL was added onto a 75 cm^2 flask of MDCK cells and incubated until Cytopathic effects were observed.

Once Cytopathic effects were observed, cells were suspended in the present media, placed in a 15 mL falcon tube, and centrifuged at max for 5 minutes. The supernatant was aspirated, leaving only about 1 mL of media in the tube. Following three -80 °C freeze and thaws it was centrifuged at max for 5 minutes. 200 μL of the supernatant was used for a viral DNA extraction (Invitrogen™ PureLink™ Viral RNA/DNA Mini Kit). Primers specific to the CAV-2 hexon were used for PCR on the extracted DNA (Table

4.2). PCR products were confirmed through gel electrophoresis. The leftover 800 μL of supernatant was used to infect a second 75 cm^2 flask of MDCK cells. Infections were carried up into a cell factory and CAV-2 was isolated using CsCl purification.

Target	**Primer**	**Sequence**
CAV-2 Hexon	F CAV-2 Hexon	5’ GGTGCACCAAGTGCCAGAGG 3’
	R CAV-2 Hexon	5’ TCACATTGGCAGGGGCCACA 3’
Amp and Ori of pAdEasy	F AdEz Amp AscI	5’ TTTGTCCTGTATATTATTGATGATGGGCGCGCCGATTCTAGTTTCGAAGCTGT 3’
	R AdEz Amp AscI	5’ TTTGTCCTGTATATTATTGATGATGGGCGCGCCATTAACATGCATGGATCCTACG 3’
Left of CAV-2 E1	F CAV-2 Mid 3	5’ GAATTAATTCCCGCGCGGCATCATCAATAATATCAGGACAAAGAGGTGT 3’
	R CAV-2 Mid 3	5’ AACGCGGAACCAGAAAATATATGAGACACAGCGAAGAGAA 3’
CMV, MCS, and pA from pShuttle-CMV	F CMV-MCS	5’ ATATTTTCTGGTTCCGCGTTACATAACTTACGT 3’
	R CMV-MCS	5’ TTTATACTCCCCGCGTTAAGATACATTGATGAGTTG 3’
Right of CAV-2 E1	F CAV-2 Right	5’ CTTAACGCGGGGAGTATAAAAGGGGCGCGG 3’
	R CAV-2 Right	5’ CCAGCCGTCCGAATTCATAGAACTATTACAGACAGACAACGC 3’
End of CAV-2 genome opposite of E1	F CAV-2 Left	5’ CTATGAATTCGGACGGCTGGCTGTCAGA 3’
	R CAV-2 Left 3	5’ TCCATGCATGGCGCGCCCATCATCAATAATATACAGGACAAAGAGGTGT 3’
Kan and Ori of pShuttle-CMV	F Kan Ori AscI	5’ ATTGATGATGGGCGCGCCGAATTAATTCGATCCTGAATGGCGAATG 3’
	R Kan Ori AscI	5’ ATTGATGATGGGCGCGCCGAATTAATTCGATCCTGAATGGCGAATG 3’

Table 4.2: This table contains all primers used within this study, along with their sequence and specific target. All primers were designed within MacVector.

pCAV-2 gDNA construction

Our genomic CAV-2 plasmid was constructed using Gibson assembly. The ampicillin resistance marker and origin of replication (Amp + Ori) were PCR amplified from pAdEasy. Primers used are listed in Table 4. 2 and were designed to have overlaps with the ends of the CAV-2 genome. The product was DpnI digested to fragment the template plasmid and then purified using Agilent Technologies StrataPrep PCR Purification Kit. Then 10 μL of purified CAV-2 was diluted in 190 μL of DPBS and Invitrogen™ PureLink™ Viral RNA/DNA Mini Kit was used to isolate the CAV-2 genomic DNA. The Amp + Ori pcr product and the genomic DNA were mixed in a 100:200 nanogram ratio. 10 μL of the 1:2 mixture was diluted into 10 μL of NEBuilder® HiFi DNA Assembly Master Mix, then incubated at 50 °C for 20 minutes. 2 μL were electroporated into electrocompetent XL-1 cells at 2500 V. Transformants were rescued in 550 μL of S.O.C media at 37°C in a shaker for 1 hour before 20 μL and 200 μL were plated onto LB + Amp plates. Single colonies were selected and grown up in 3 mL of LB + Amp media. Plasmid DNA was isolated from the bacterial samples (QIAprep Spin Miniprep Kit) following manufacturer's protocol. Plasmid DNA was AscI (NEB) digested and the product was confirmed through gel electrophoresis. Plasmid construction was further confirmed through PCR specific for the CAV-2 hexon and whole plasmid sequencing available through Eurofins genomics.

ΔE1 CAV-2 Shuttle Plasmid Development

Our ΔE1 CAV-2 Shuttle Plasmid was developed utilizing a combination of overlapping PCR and Gibson assembly. All fragments required for shuttle construction include the

500 bps left of CAV-2 E1 (Left E1), a major cloning site (MCS) flanked by a CMV promoter and polyadenylation signal (CMV MCS), 500 bps right of CAV-2 E1 (Right E1), the 500 bps at the end of the CAV-2 genome (End CAV-2), and a fragment containing a kanamycin resistance gene (kan) plus an origin of replication (ori) (Kan + ori). First the Left E1, CMV MCS, right E1, and End CAV-2 were PCR amplified using Q5 high fidelity DNA polymerase (NEB). All primers used are listed in Table 4.2 and were designed to include overlaps to the fragments adjacent in the final product. All four PCR products were confirmed through gel electrophoresis and gel extracted (QIAquick Gel Extraction Kit). The gel extracted products were then mixed in an equal molar ratio for overlapping PCR. The kan + ori was PCR amplified from pShuttle-CMV then DpnI digested to fragment any remaining shuttle plasmid template. The overlapping PCR product and the Kan + Ori fragment were mixed in a 2:1 ratio. 10 μL of NEBuilder® Hifi DNA Assembly 2X Master Mix was added to the tube and incubated at 50°C for 20 minutes. 2 μL of the Gibson assembly product was transformed into XL-1 cells. Transformants were rescued in 550 μL of S.O.C media at 37°C in a shaker for 1 hour before 20 μL and 200 μL were plated onto LB + Kan plates. Single colonies were selected and grown up in 3 mL of LB + Kan media. Plasmid DNA was isolated from the bacterial samples (QIAprep Spin Miniprep Kit) and screened through AscI digest and whole plasmid sequencing available through Eurofins genomics.

CHAPTER 5: CONCLUSIONS AND FUTURE DIRECTIONS

In this thesis we have outlined our developmental approach for a potentially broadly protective Canine Influenza Vaccine. Canine Influenza Virus (CIV), a recently emerged branch of Influenza A virus, is most often known to cause coughing, fever, and tracheobronchitis in dogs, with severe cases leading to pneumonia and death [17, 99]. Due to the relatively short history, and slower evolution rates, the reported diversity within both the H3N8 and H3N2 variants does not eclipse 10% [27]. Therefore, we theorize that if a vaccine is developed that can protect against most CIV variants while it has limited diversity, then CIV can potentially be eliminated before it becomes more diverse and unmanageable. Currently available commercial vaccines use outdated strains for their inactivated influenza virus cocktails, causing the recently observed drop in vaccine effectiveness [38, 58]. Beyond the current vaccines simply being outdated, inactivated influenza vaccines, in general, are often strain specific, and report poor protection against viruses heterologous to the vaccine strains [4]. Therefore, we are working to develop a vaccine that can induce broad protection against many CIV variants.

The Mosaic Vaccine designer works to create a broadly protective vaccine immunogen from a population of natural sequences. This vaccine designer relies on an in silico algorithm to generate a recombinant sequence with the highest percentage of potential T cell epitopes [61]. The major benefit in utilizing a mosaic immunogen, rather than updating current vaccines with new strains, is that the mosaic immunogens are intentionally biased towards T cell responses [61]. Inactivated influenza vaccines (IIV), such as the ones currently available for CIV, tend to elicit very strong, strain specific

humoral responses, but inefficient CD8+ T cell responses [4]. Consequently, as cell mediated immunity is generally more cross-protective against influenza than humoral immunity, IIVs provide poor protection to mismatched strains [4] A mosaic immunogen also has an edge on a consensus immunogen. The consensus approach does not consider common or unnatural potential T cell epitopes during development, while the mosaic algorithm will eliminate unnatural epitopes, while incorporating common theoretical T cell epitopes [61]. As cell mediated immunity against influenza is generally more cross reactive than humoral immunity, we utilized the mosaic vaccine designer to develop a mosaic canine influenza hemagglutinin (CanH3 mosaic) as our vaccine immunogen. Previous studies developing a mosaic H1 and H5 vaccine have demonstrated the ability of these mosaic immunogens to induce broad protection in mice [62, 64]. We theorize our CanH3 mosaic could have similar or even broader impacts.

Phylogenetic analysis of our generated mosaic immunogen revealed it had localized centrally within H3N2 HA sequences, with a maximum of 5% divergence between the CanH3 mosaic and any other H3N2 HA sequences. We thereby hypothesize that our immunogen will have broad coverage for H3N2 sequences. However, protection from the H3N8 subtype could suffer because of this, as our canH3 mosaic only boasts around 85% similarity with H3N8 HA sequences. This issue could be minimized by adding a second mosaic HA generated with only H3N8 sequences, but since H3N2 is the predominantly circulating subtype of CIV and H3N8 has not been reported post-2016, we predict this may not be necessary. A future resurgence of H3N8 remains a potential drawback to our vaccine design. Future strains of H3N2 CIV also present a potential setback to our mosaic immunogen, as influenza can quickly mutate and produce immune escape

variants. We predict our CanH3 mosaic immunogen will provide broader immune protection against these future strains than commercial comparators because mosaic design is biased towards the more broadly protective cell mediated immune response. If protection does wane against future strains, an updated mosaic vaccine can be produced within 2-6 months.

To deliver our immunogen, we plan to utilize both a human Adenovirus type 5 and Canine Adenovirus Type 2 Vector. Through the pAdEasy system, we were able to insert the CanH3 mosaic into HAd5 and grow recombinant virus. The presence of our transgene within our recombinant virus was confirmed with PCR, so the next step involves confirming expression of the CanH3 mosaic within infected cells. It is fundamental that our vaccine can induce transgene expression, or it will not be able to induce any immunity against CIV. Therefore, confirming expression remains a priority before we can move on with future studies. Regarding CAV-2, a vector system is not commercially available, so we developed both CAV-2 genomic and shuttle plasmids that we can theoretically use to generate recombinant CAV-2. Gibson assembly appears to be quite effective when ligating together only two fragments, as that was the primary method in developing our genomic CAV-2 plasmid. However, efficiency of Gibson assembly diminished when trying to ligate together more than two fragments. We initially planned to only use Gibson assembly to develop our CAV-2 shuttle plasmid, but we had no success in ligating together all five required fragments within one reaction. We therefore relied on overlapping PCR to ligate the majority of the fragments before finishing the plasmid construction with Gibson assembly. A combination of both methods could be a potentially efficient method for constructing recombinant plasmids. We have yet to

demonstrate that these plasmids can generate recombinant CAV-2. Therefore, future efforts remain focused on inserting a transgene into the shuttle vector and co-transforming with pCAV-2 gDNA to generate a recombinant CAV-2 genome through homologous recombination. It is essential to confirm whether this recombinant CAV-2 genome can produce recombinant virus, as it is one of the vectors we plan to use to deliver our mosaic immunogen. We will confirm this by transfecting linearized recombinant CAV-2 genomic, containing our mosaic immunogen expression cassette, into MDCK cells and observe for CPE. We will then assess expression of our mosaic through western blots to ensure our recombinant CAV-2 can express our vaccine immunogen.

After constructing both of our adenoviral vectored vaccines, and confirming transgene expression, we plan to move our studies in to mouse models. Mouse models are very popular models for influenza research, as mice are relatively cheap and easy to handle [100]. Since influenza does not naturally infect these mice, strains often must be mouse-adapted before use [100]. Regardless, mouse models are often useful for obtaining preliminary insight into the effectiveness of vaccines [100]. We would like to assess the effectiveness of our vaccines compared to commercially available vaccines through challenge studies and immune correlates from mice. To assess the antibody response, we would utilize hemagglutinin inhibition assays. This assay attempts to measure HA inhibiting antibodies by determining the highest dilution of sera that can prevent red blood cell agglutination [13, 60]. An HI titer of 40 or higher is general standard of protection and would be a promising result, but ideally, the mosaic would have to induce higher HI titer higher than the commercial comparator for any CIV strains tested [13, 60].

To assay T cell responses, we would utilize IFN-γ elispot assays. This would allow us to gauge relative T cell responses, and we expect our mosaic immunogen to outperform commercial comparators as its development is biased towards CD8+ T cell responses. Having two separately vectored adenoviral systems will allow us to compare the effectiveness between them and evaluate the effect serotype switching has on inducing protection. If results are promising, an eventual move into dog models will be warranted. It will be important to determine whether vaccination induces sterilizing immunity or just prevents disease, as homologous recombination can occur if the virus can replicate, even at low levels. By collecting nasal swabs during CIV challenge, we can determine the presence of viral RNA and infectious virus through RT-PCR and determining $TCID_{50}$ (Mean tissue culture infectious dose). If vaccination with our mosaic induces sterilizing immunity, we would expect both results to be similar to a negative control. If sterilizing immunity is not induced, it would be essential to determine if our mosaic vaccine can, at minimum, prevent the spread of CIV between hosts. One potential limitation on these studies is the availability of CIV strains, which are not often obtainable through most distributors and must be obtained through collaboration or veterinary diagnostic centers. We could potentially generate a CIV surrogate through reverse genetics, but natural strains would be preferable.

In summary, CIV remains an ever-present issue for not only dogs, but humans as well. The close proximity dogs have with humans as companion animals provides the perfect opportunity for cross species transmission. The risk does not end there, because in the two decades since the discovery of the virus, CIV reassortments with swine and avian influenza A strains have already been observed in dogs [30, 42, 43]. This showcases the

potential threat that dogs could serve as “mixing bowls” for the emergence of novel influenza A viruses. The 2009 swine flu pandemic paints a perfect picture of the dangers that result from these mixing bowls, as the reassorted H1N1 pandemic strain infected over 24% of the global population [5]. This highlights the need for the development of a new vaccine strategies in canines, to protect dogs from respiratory ailments and to prevent the emergence of novel reassorted Influenza A viruses.

REFERENCES

1. *Center for Disease Control and Prevention: Disease Burden of Flu*. 2022 [cited 2023 10/20/2023]; Available from: https://www.cdc.gov/flu/about/burden/index.html
2. Wayan C.W.S. Putri a b, D.J.M.a., Melissa S. Stockwell c, Anthony T. Newall *Economic burden of seasonal influenza in the United States.* Vaccine, 2018. **36**(27): p. 3960-3966.
3. Weir, J.P. and M.F. Gruber, *An overview of the regulation of influenza vaccines in the United States.* Influenza Other Respir Viruses, 2016. **10**(5): p. 354-60.
4. Jansen, J.M., et al., *Influenza virus-specific CD4+ and CD8+ T cell-mediated immunity induced by infection and vaccination.* J Clin Virol, 2019. **119**: p. 44-52.
5. Van Kerkhove, M.D., et al., *Estimating age-specific cumulative incidence for the 2009 influenza pandemic: a meta-analysis of A(H1N1)pdm09 serological studies from 19 countries*. 2009.
6. Shao, W., et al., *Molecular Sciences Evolution of Influenza A Virus by Mutation and Re-Assortment*.
7. Chen, J.R., et al., *Better influenza vaccines: an industry perspective.* J Biomed Sci, 2020. **27**(1): p. 33.
8. Nyirenda, M., et al., *Estimating the Lineage Dynamics of Human Influenza B Viruses.* PLOS ONE, 2016. **11**(11): p. e0166107.
9. Gilbertson, B., M. Duncan, and K. Subbarao, *Role of the viral polymerase during adaptation of influenza A viruses to new hosts.* Curr Opin Virol, 2023. **62**: p. 101363.
10. Chauhan, R.P. and M.L. Gordon, *An overview of influenza A virus genes, protein functions, and replication cycle highlighting important updates.* Virus Genes, 2022. **58**(4): p. 255-269.
11. Krammer, F., et al., *Influenza*, in *Nature Reviews Disease Primers*. 2018, Nature Publishing Group. p. 1-21.
12. Samji, T., *Influenza A: Understanding the Viral Life Cycle*, in *YALE JOURNAL OF BIOLOGY AND MEDICINE*. 2009. p. 153-159.
13. Wu, N.C. and I.A. Wilson, *Influenza Hemagglutinin Structures and Antibody Recognition*. 2020.
14. Eisfeld, A.J., G. Neumann, and Y. Kawaoka, *At the centre: influenza A virus ribonucleoproteins.* Nat Rev Microbiol, 2015. **13**(1): p. 28-41.
15. Crawford, P.C., et al., *Transmission of Equine Influenza Virus to Dogs*. 2005. p. 482-485.
16. Song, D., et al., *Transmission of Avian Influenza Virus (H3N2) to Dogs*. 2008. p. 741.
17. Parrish, C.R., I.E.H. Voorhees, and *H3N8 and H3N2 Canine Influenza Viruses: Understanding These New Viruses in Dogs*. 2019. p. 643-649.
18. Xie, X., K. Ma, and Y. Liu, *Influenza A virus infection in dogs: Epizootiology, evolution and prevention - A review.* Acta Vet Hung, 2016. **64**(1): p. 125-39.
19. Dubovi, E.J., *Canine influenza.* Vet Clin North Am Small Anim Pract, 2010. **40**(6): p. 1063-71.

20. Zhou, P., et al., *Seroepidemiological Evidence of Subtype H3N8 Influenza Virus Infection among Pet Dogs in China*. 2016, Public Library of Science. p. e0159106.
21. Pecoraro, H.L., et al., *Epidemiology and Ecology of H3N8 Canine Influenza Viruses in US Shelter Dogs*. 2014.
22. Dalziel Benjamin D. AND Huang, K.A.N.D.G.J.L.A.N.D.A.N.A.N.D.D.E.J.A.N.D.G.B.T.A.N. and *Contact Heterogeneity, Rather Than Transmission Efficiency, Limits the Emergence and Spread of Canine Influenza Virus*. 2014, Public Library of Science. p. 1-13.
23. Voorhees, I.E.H., et al., *Multiple Incursions and Recurrent Epidemic Fade-Out of H3N2 Canine Influenza A Virus in the United States*. 2018, American Society for Microbiology.
24. Barrell, E.A., et al., *Seroprevalence and Risk Factors for Canine H3N8 Influenza Virus Exposure in Household Dogs in Colorado*. 2010.
25. Zhu, H., J. Hughes, and P.R. Murcia, *Origins and Evolutionary Dynamics of H3N2 Canine Influenza Virus.* Journal of Virology, 2015. **89**(10): p. 5406-5418.
26. He, W., et al., *Emergence and adaptation of H3N2 canine influenza virus from avian influenza virus: An overlooked role of dogs in interspecies transmission.* Transboundary and Emerging Diseases, 2019. **66**(2): p. 842-851.
27. Zhu, H., J. Hughes, and P.R. Murcia, *Origins and Evolutionary Dynamics of H3N2 Canine Influenza Virus*. 2015, American Society for Microbiology. p. 5406-5418.
28. Klivleyeva, N.G., et al., *Influenza A viruses circulating in dogs: A review of the scientific literature*. 2022, Faculty of Veterinary Medicine, University of Tripoli. p. 676.
29. Su, S., et al., *Avian-origin H3N2 canine influenza virus circulating in farmed dogs in Guangdong, China*. 2013, Elsevier. p. 444-449.
30. Chen, Y., et al., *Emergence and Evolution of Novel Reassortant Influenza A Viruses in Canines in Southern China*. 2018.
31. Rovid Spickler, A. and *Canine Influenza*. 2007.
32. Lyu, Y., et al., *Canine Influenza Virus A(H3N2) Clade with Antigenic Variation, China, 2016–2017*. 2019, Centers for Disease Control and Prevention. p. 161.
33. Sun, Y., et al., *A serological survey of canine H3N2, pandemic H1N1/09 and human seasonal H3N2 influenza viruses in dogs in China*. 2014, Elsevier. p. 193-196.
34. Su, W., et al., *Seroprevalence of dogs in Hong Kong to human and canine influenza viruses*. 2019, John Wiley & Sons, Ltd. p. e000327.
35. Zhang, Y.-B., et al., *Serologic Reports of H3N2 Canine Influenza Virus Infection in Dogs in Northeast China*.
36. Li, Y., et al., *Characterization of canine influenza virus a (H3n2) circulating in dogs in china from 2016 to 2018*. 2021, MDPI. p. 2279.
37. Voorhees, I.E.H., et al., *Spread of Canine Influenza A(H3N2) Virus, United States.* Emerg Infect Dis, 2017. **23**(12): p. 1950-1957.
38. Xu, W., et al., *Phylogenetic Inference of H3N2 Canine Influenza A Outbreak in Ontario, Canada in 2018*. 2020, Nature Publishing Group.

39. Jang, H., et al., *Seroprevalence of three influenza A viruses (H1N1, H3N2, and H3N8) in pet dogs presented to a veterinary hospital in Ohio*. 2017, The Korean Society of Veterinary Science. p. 291-298.
40. Ma, W., R.E. Kahn, and J.A. Richt, *The pig as a mixing vessel for influenza viruses...* 2009. p. 158-166.
41. Thongratsakul, S., et al., *Avian and human influenza A virus receptors in trachea and lung of animals*.
42. Meng, B., et al., *Emergence of a novel reassortant H3N6 canine influenza virus.* Front Microbiol, 2023. **14**: p. 1186869.
43. Song, D., et al., *A novel reassortant canine H3N1 influenza virus between pandemic H1N1 and canine H3N2 influenza viruses in Korea*. 2012, Microbiology Society. p. 551.
44. Chen, Y., et al., *Dogs are highly susceptible to H5N1 avian influenza virus*. 2010, Academic Press Inc. p. 15-19.
45. Lin, H.T., et al., *Influenza A(H6N1) Virus in Dogs, Taiwan*. 2015, Centers for Disease Control and Prevention. p. 2154.
46. Guang-jian, Z., et al., *Genetic characterization of a novel influenza A virus H5N2 isolated from a dog in China*. 2012, Vet Microbiol. p. 409-416.
47. Sun, X., et al., *Evidence of avian-like H9N2 influenza A virus among dogs in Guangxi, China*. 2013, Elsevier B.V. p. 471-475.
48. Lin, D., et al., *Natural and experimental infection of dogs with pandemic H1N1/2009 influenza virus*. 2012, Microbiology Society. p. 119-123.
49. *History of the Influenza Vaccine*. November 3, 2023]; Available from: https://www.who.int/news-room/spotlight/history-of-vaccination/history-of-influenza-vaccination.
50. Taubenberger, J.K., J.V. Hultin, and D.M. Morens, *Discovery and characterization of the 1918 pandemic influenza virus in historical context*. 2007, National Institude of Allergy and Infectious Diseases, National Institutes of Health, Bethesda, MD, USA. p. 581-591.
51. Nypaver, C., C. Dehlinger, and C. Carter, *Influenza and Influenza Vaccine: A Review*. 2021, J Midwifery Womens Health. p. 45-53.
52. Yamayoshi, S. and Y. Kawaoka, *Current and future influenza vaccines.* Nat Med, 2019. **25**(2): p. 212-220.
53. Yatim, K.M. and F.G. Lakkis, *A brief journey through the immune system.* Clin J Am Soc Nephrol, 2015. **10**(7): p. 1274-81.
54. Herwald, H. and A. Egesten, *On PAMPs and DAMPs.* J Innate Immun, 2016. **8**(5): p. 427-8.
55. *The innate and adaptive immune systems [Updated 2020 Jul 30]*. Available from: https://www.ncbi.nlm.nih.gov/books/NBK279396/?report=classic.
56. *Vanguard® CIV H3N2/H3N8 | Zoetis US*.
57. *Compendium of Veterinary Products - Nobivac® Canine Flu Bivalent (MERCK ANIMAL HEALTH)*.
58. Scott Weese, J., et al., *Emergence and Containment of Canine Influenza Virus A(H3N2), Ontario, Canada, 2017–2018*. 2019, Centers for Disease Control and Prevention. p. 1810.

59. Feng, J., et al., *Antibody quantity versus quality after influenza vaccination.* Vaccine, 2009. **27**(45): p. 6358-62.
60. Allen, J.D. and T.M. Ross, *H3N2 influenza viruses in humans: Viral mechanisms, evolution, and evaluation.* Hum Vaccin Immunother, 2018. **14**(8): p. 1840-1847.
61. Fischer, W., et al., *Polyvalent vaccines for optimal coverage of potential T-cell epitopes in global HIV-1 variants.* Nature Medicine, 2007. **13**(1): p. 100-106.
62. Kamlangdee, A., et al., *Mosaic H5 Hemagglutinin Provides Broad Humoral and Cellular Immune Responses against Influenza Viruses.* Journal of Virology, 2016.
63. Bullard, B.L., et al., *Strategies Targeting Hemagglutinin as a Universal Influenza Vaccine*. 2021.
64. Corder, B.N., et al., *Influenza H1 Mosaic Hemagglutinin Vaccine Induces Broad Immunity and Protection in Mice*. 2019.
65. Sayedahmed, E.E., et al., *Adenoviral Vector-Based Vaccine Platforms for Developing the Next Generation of Influenza Vaccines.* Vaccines (Basel), 2020. **8**(4).
66. Coughlan, L., C. Mullarkey, and S. Gilbert, *Adenoviral vectors as novel vaccines for influenza.* J Pharm Pharmacol, 2015. **67**(3): p. 382-99.
67. Zhou, S., et al., *A simplified system for generating recombinant adenoviruses*, in *Medical Sciences*. 1998. p. 2509-2514.
68. Chang, J., *Adenovirus vectors: Excellent tools for vaccine development*. 2021, Korean Association of Immunologists. p. 1-11.
69. Kulanayake, S. and S.K. Tikoo, *Adenovirus Core Proteins: Structure and Function.* Viruses, 2021. **13**(3).
70. Watanabe, M., et al., *Adenovirus Biology, Recombinant Adenovirus, and Adenovirus Usage in Gene Therapy.* Viruses, 2021. **13**(12).
71. Schuldt, N.J., et al., *Immunogenicity when utilizing adenovirus serotype 4 and 5 vaccines expressing circumsporozoite protein in nave and Adenovirus (Ad5) immune mice.* Malaria Journal, 2012. **11**.
72. Sayedahmed, E.E., et al., *Longevity of adenovirus vector immunity in mice and its implications for vaccine efficacy.* Vaccine, 2018. **36**(45): p. 6744-6751.
73. Ternovoi, V.V., et al., *Productive replication of human adenovirus type 5 in canine cells.* J Virol, 2005. **79**(2): p. 1308-11.
74. Zhao, Z., et al., *Recombinant Human Adenovirus Type 5 Co-expressing RABV G and SFTSV Gn Induces Protective Immunity Against Rabies Virus and Severe Fever With Thrombocytopenia Syndrome Virus in Mice.* Front Microbiol, 2020. **11**: p. 1473.
75. Yan, L., et al., *A Bivalent Human Adenovirus Type 5 Vaccine Expressing the Rabies Virus Glycoprotein and Canine Distemper Virus Hemagglutinin Protein Confers Protective Immunity in Mice and Foxes.* Front Microbiol, 2020. **11**: p. 1070.
76. Vos, A., et al., *Immunogenicity of an E1-deleted recombinant human adenovirus against rabies by different routes of administration*, in *Journal of General Virology*. 2001. p. 2191-2197.
77. Kovesdi, I. and S.J. Hedley, *Adenoviral producer cells.* Viruses, 2010. **2**(8): p. 1681-1703.
78. Ison, M.G. and R.T. Hayden, *Adenovirus.* 2016.

79. Ip, W.H. and T. Dobner, *Cell transformation by the adenovirus oncogenes E1 and E4.* FEBS Lett, 2020. **594**(12): p. 1848-1860.
80. Decaro, N., V. Martella, and C. Buonavoglia, *Canine adenoviruses and herpesvirus.* Vet Clin North Am Small Anim Pract, 2008. **38**(4): p. 799-814, viii.
81. Zhu, Y., et al., *Difference Analysis Between Canine Adenovirus Types 1 And 2.* Front Cell Infect Microbiol, 2022. **12**: p. 854876.
82. Bouet-Cararo, C., et al., *Canine adenoviruses elicit both humoral and cell-mediated immune responses against rabies following immunisation of sheep*. 2011, Elsevier. p. 1304-1310.
83. Zhang, S., et al., *Oral vaccination of dogs (Canis familiaris) with baits containing the recombinant rabies-canine adenovirus type-2 vaccine confers long-lasting immunity against rabies*. 2008, Elsevier. p. 345-350.
84. Li, J., et al., *A single immunization with a recombinant canine adenovirus expressing the rabies virus G protein confers protective immunity against rabies in mice*. 2006, Academic Press. p. 147-154.
85. Henderson, H., et al., *Oral immunization of raccoons and skunks with a canine adenovirus recombinant rabies vaccine*. 2009. p. 7194-7197.
86. Fischer, L., et al., *Vaccination of puppies born to immune dams with a canine adenovirus-based vaccine protects against a canine distemper virus challenge*. 2002. p. 3485-3497.
87. Tu, L., et al., *Evaluation of protective efficacy of three novel H3N2 canine influenza vaccines.* 2017. p. 98084-98093.
88. De Vleeschauwer, A.R., et al., *A canine adenovirus type 2 vaccine vector confers protection against foot-and-mouth disease in guinea pigs*. 2018, Elsevier Ltd. p. 2193-2198.
89. AU - Szelechowski, M., et al., *Production and Purification of Non Replicative Canine Adenovirus Type 2 Derived Vectors*. 2013, MyJoVE Corp. p. e50833.
90. Gibson, D.G., et al., *Enzymatic assembly of DNA molecules up to several hundred kilobases.* Nature Methods 2009 6:5, 2009. **6**(5): p. 343-345.
91. Pan, H., et al., *Rapid Construction of a Replication-Competent Infectious Clone of Human Adenovirus Type 14 by Gibson Assembly*. 2018, Multidisciplinary Digital Publishing Institute (MDPI).
92. *Gibson Assembly: An overview of Gibson Assembly,, a techniue to creation exceptionally large molecular clones from PCR products*. [cited 2022 10/23/2023]; Available from: https://www.snapgene.com/guides/gibson-assembly.
93. Grable, M. and P. Hearing, *Adenovirus Type 5 Packaging Domain Is Composed of a Repeated Element That Is Functionally Redundant*, in *JOURNAL OF VIROLOGY*. 1990. p. 2047-2056.
94. Davison, A.J., M. Benko, and B. Harrach, *Genetic content and evolution of adenoviruses.* J Gen Virol, 2003. **84**(Pt 11): p. 2895-2908.
95. Ahi, Y.S. and S.K. Mittal, *Components of Adenovirus Genome Packaging.* Front Microbiol, 2016. **7**: p. 1503.
96. Hoeben, R.C. and T.G. Uil, *Adenovirus DNA replication.* Cold Spring Harb Perspect Biol, 2013. **5**(3): p. a013003.

97. Wright, N., et al., *High prevalence of antibodies against canine adenovirus (CAV) type 2 in domestic dog populations in South Africa precludes the use of CAV-based recombinant rabies vaccines*. 2013. p. 4177-4182.
98. Bulut, O., et al., *The serological and virological investigation of canine adenovirus infection on the dogs*. 2013.
99. *Key Facts about Canine Influenza (Dog Flu) | Seasonal Influenza (Flu) | CDC*.
100. Nguyen, T.Q., R. Rollon, and Y.K. Choi, *Animal Models for Influenza Research: Strengths and Weaknesses*. 2021, Multidisciplinary Digital Publishing Institute (MDPI).